2019

Evaluating the Use of sUAS-Derived Imagery for Monitoring Flood Protection Infrastructure

Eleanor Mei Dietz
University of Mississippi

EVALUATING THE USE OF sUAS-DERIVED IMAGERY FOR MONITORING FLOOD PROTECTION INFRASTRUCTURE

A Thesis

Presented in partial fulfillment of the requirements

For the degree of Master of Science

In the Department of Geology and Geological Engineering

The University of Mississippi

By

Eleanor M. Dietz

May 2019

ABSTRACT

In the US there are approximately 33,000 miles of levees. This includes 14,500 miles of levee systems associated with US Army Corps of Engineers programs and approximately 15,000 miles from other state and federal agencies. More than 14 million people live behind levees and associated flood prevention infrastructure. Monitoring and risk assessment are an on-going process, especially during times of flood conditions. The city of New Orleans was heavily impacted by Hurricane Katrina in 2005 by storm surges and intense rainfall. The impact of the hurricane was substantial enough to cause levee failure and I-wall toppling where many of the levees were breached and waters flooded the city. Subsidence and increasing population are likely to make flooding events more frequent and costly. As new technologies emerge, monitoring and risk assessment can benefit to increase community resiliency.

In this research, I investigate the use of the *structure from motion* photogrammetric method to monitor positional changes in invariant objects such as levees, specifically, I-walls. This method uses conventional digital images from multiple view locations and angles by either a moving aerial platform or terrestrial photography. Using parallel coded software and accompanying hardware, 3D point clouds, digital surface models and orthophotos can be created. By providing comparisons of similar processing workflows with a variety of imaging acquisition criteria using commercially available unmanned aerial systems (UAS), we created multiple image sets of a simulated I-wall at various flight elevations, look angles, and effective overlap. The comparisons can be used for sensor selection and mission planning to improve the quality of the final product.

DEDICATION

To the peaceful application of photogrammetry in order to maximize the scientific, social, and commercial benefits of this technology for all humankind.

LIST OF ABBREVIATIONS

DEM	Digital Elevation Model
FAA	Federal Aviation Administration
GCP	Ground Control Point
GDAL	Geodata Analysis Laboratory
GIS	Geographic Information System
GNSS	Global Navigation Satellite System
GPS	Global Positioning Satellite
GSD	Ground Sampling Distance
GUI	Graphical User Interface
IMU	Inertial Measurement Unit
IPET	Interagency Performance Evaluation Task Force
LAS	Laser file format
LiDAR	Light Detection and Ranging
RTK	Real Time Kinematic
SfM	Structure from Motion
SIFT	Scale-Invariant Feature Transform
TLS	Terrestrial Laser Scanning
UAS	Unmanned Aerial Systems
UMFS	University of Mississippi Field Station
UNAVCO	University NAVSTAR Consortium
USACE	United States Army Corps of Engineers

ACKNOWLEDGMENTS

There are many people I would like to recognize who have helped a great deal with my research. First and foremost, I would like to thank The University of Mississippi Department of Geology and Geological Engineering for providing a home for my studies and financial support for this project. I would also like to thank the folks at The University of Mississippi Field Station for letting me use the land for my research.

Very special thanks goes to my main advisor, Dr. Lance Yarbrough who gave me the opportunity to carry out this project and involved me in many other projects that have improved my knowledge in this field immensely. I truly appreciate your guidance and insight. Also, to my committee members, Dr. Greg Easson, and Dr. Louis Zachos, who directed me during my research. I am indebted to you all for your assistance and patience with my work.

I would like to express my appreciation to my fellow graduate students for helping me along the way. Thank you for your friendship.

Finally, I would like to thanks my family and friends back home who have encouraged and supported me along the way. To my parents, mom and dad, who have supported me along the years and provided me with my every need and more, thank you.

TABLE OF CONTENTS

LIST OF TABLES

LIST OF FIGURES

CHAPTER I

INTRODUCTION

The rise in the development and availability of unmanned aerial systems (UAS) has led to a wide array of applications for geologic research. The smaller size and simplicity, as compared to more traditional equipment, has made UAS more valuable in areas such as slope monitoring, surveillance, and forward modeling of scenarios (Fraser et al., 2019). UAS offer a unique opportunity to study places that are otherwise challenging or impossible access with low operational costs. Unmanned aircraft systems can be modified to suit the different needs of data collection; they are also capable of collecting and transmitting information from inaccessible areas (Madden et al., 2015). For the purposes of this study, the UAS classification is focused mainly on micro to small size UAS, larger, more commercial UAS will not be applied in this research. After post-processing, image data will provide a 3D model that can help visualize changes to the object in question. In this study, UAS acquired images are used to assess small displacements made by a vertical mock I-wall. The images are then processed and analyzed in a photogrammetric solutions system, using structure from motion (SfM).

A levee is described as a “man-made structure; usually an earthen embankment, designed and constructed in accordance with sound engineering practices to contain, control, or divert the flow of water to provide protection from temporary flooding” (FEMA Resources, 2017). A typical levee is composed of a toe, crown, berm, and slopes. The crown is the flat area sitting on top of the levee while the toe is the edge of the levee where it meets the natural ground. When designing a levee, multiple factors are considered such as construction, environmental conditions, local geology and vegetation, risk of flooding, and types of material to cover the levee (Lee, 2010). In the US, the United States Army Corps of Engineers (USACE) controls and maintains levee systems with continual safety assessments. There are many US levee systems that are nearing their life of design where they become more susceptible to the severity of increasing storms, therefore it is crucial to constantly monitor and assess the stability of levees (Fisher, 2016).

Levees breached in New Orleans August 29, 2005 as a result of Hurricane Katrina as it passed through the city (Duncan et al., 2008). During a large flood event, levees may breach and lead to the inundation of large areas and cause concern for property and loss of life. A large portion of the destruction from the Hurricane Katrina in New Orleans was caused by policy-related engineering failures and complacency of construction (van Heerden, 2006). Many poor, construction decisions were made during the creation of these levees and floodwalls (Lee, 2010). Understanding the modes of failure, efforts can be aimed towards mitigating any possible future effects of hurricane and I-walls can be managed more properly.

An I-wall is a reinforced concrete wall panel built atop sheet piling, usually found above levees to cut off flow of water beneath the wall (Seed et al., 2008). The purpose of an I-wall is to prevent flooding into areas that have been developed by raising the height of the levee. The I-walls raise the level of flood protection without expanding the width of the physical levee (Duncan et al., 2008). During Hurricane Katrina, many I-walls failed because there was a lack of proper care and maintenance of the levees and the magnitude of destruction the storm brought were not anticipated (Sills et al., 2008). The I-wall design used in New Orleans did not account for variability of strength for the soft soils beneath the levees which were not armored for a storm of this magnitude. This led to conditions where water filled the gap, formed by a crack, behind the I-walls and floodwaters exerted forces that toppled the I-walls which then triggered an erosion process of the highly erodible soil (Ubilla et al., 2008). This soil sloughed off and allowed water to pour into the city of New Orleans. The research stemmed from these I-wall failures during Hurricane Katrina and investigates a way to monitor for displacements as a precursor to failure modes. The key issue is whether or not a vertical wall can be seen moving out of alignment through a point cloud. This is done by performing a point cloud comparison to see which parameters work best for this research to define a clear edge of an I-wall.

This study provides a workflow for detailed and repeatable methods to construct a 3D model of a simulated I-wall to test the use of UAS imagery and SfM as a tool to monitor flood control structures. Proper photogrammetry techniques can be used to help assess the toppling of any levee system and monitor the state of current walls. Using a UAS, the user can define an effective solution, with the aid of a few ground control points (GCP), by point cloud comparison. This proposed method is ideal for applications where a UAS can acquire a small level of detection in movement through point cloud comparisons. In ideal conditions, this type of approach to a project of this magnitude can be increased and improved upon to increase the level of detection in larger areas. The application of this project is to compare point cloud differences and define the edge of the I-wall even if outliers are present.

This study is an investigation on the feasibility of UAS as a survey tool to note and predict movement a mock I-wall. The capabilities of UAS are endless and growing with the rise in technology. UAS can be comparable to terrestrial laser scanning (TLS) because of its ability to generate high point densities. The millimeter level accuracy that is attained by the final dense point clouds in Agisoft Photoscan by UAS photogrammetry is equally comparable as long range

TLS. These SfM principles could possibly be improved by Light Detection and Ranging (LiDAR) but is a match for the current UAS system from this study. To ensure consistency, the UAS will need a mission planning software to securely and rapidly execute the flight acquisition. For smaller areas, such as the one performed in this study, the flight acquisition can be very simple, swift, and affordable. Larger areas may require more equipment that can sustain a longer battery life.

The goal of this research is to investigate the use of UAS acquired imagery as a tool to monitor the stability and conditions of I-wall levee system. This is done by:

- Characterize temporal data where correlation of images taken at separate times are used to monitor dynamic changes of a floodwall structure.
- Use SfM methods to detect possible movement of an I-wall or flood control structure
    - This can be accomplished by using a scaled down version of one particular I-wall, constructed by using wood panels and plywood that can be manipulated for different data sets.
- A sensitivity analysis test of the UAS to determine optimal aircraft to target the orientation of a panel or target a reflective structure.
- A multispectral analysis will be performed to see if the integration of this type of data could improve the detection of I-wall movement.

Combining UAS with SfM, images can be captured in hard to reach places, areas that cannot be captured by traditional terrestrial methods. These images can be used to construct a 3D model that may be able to improve survey operations. Using SfM with post-processing software, Agisoft, a 3D point cloud and digital elevation model (DEM) can be created. With this process, the goal is to detect lean or movement using the UAS. More specifically, the UAS may be able to detect the lean angle and direction using the top of a model I-wall. With these data, predictions can be made of any indication of potential failures or slump failures. Based on all the information given, a prognosis can determine if a specific site is vulnerable to extreme weather conditions for geohazard mitigation.

CHAPTER II

BACKGROUND

General Levee Construction

Levees are a type of raised embankment designed to an elevation to reduce the risk of flooding and seasonal high water to an area (USACE, 2000). These structures are not deformed or reshaped under normal water conditions, such as current or waves, because their primary purpose is to provide protection against flooding. Historically, levees were built to reduce the risk of flooding, defined by the water level given in previous historic floods (Seed, 2008). This design method only considers a single variable for flood protection rather than the several variables that make up a flood risk management system. Newer levee designs consider numerous input variables such as property or settlement downstream from the levee, economic viability of the design, and consequences due to strength of material below the levee. Thorough investigations and proper operational standards are made to consider all factors.

If levees are not maintained properly, they can deteriorate over time and require more maintenance. Flood defense systems include flood walls, I-walls, pumping stations, closing gates, natural features, levees, and other associated features (London, 2013). Figure 1 illustrates the general design of a levee with each component labeled. Each component of the system must perform competently to achieve optimal design effectiveness. A levee fails when it does not reach its desired performance outcome within a given set of parameters, or when water flows through (USACE, 2000). Since levees are very complex, there are numerous variables that must be investigated before building a levee. Major requirements call for a thorough geologic analysis, a subsurface foundational analysis, and then the embankment parameters are defined with the known strength numbers of the foundation materials (Comfort, 2006). Each section of levee is examined for underseepage, slope stability, and settlement. In addition, the method of levee construction, effective adaptation, and routine maintenance schedules must be considered (London, 2013).

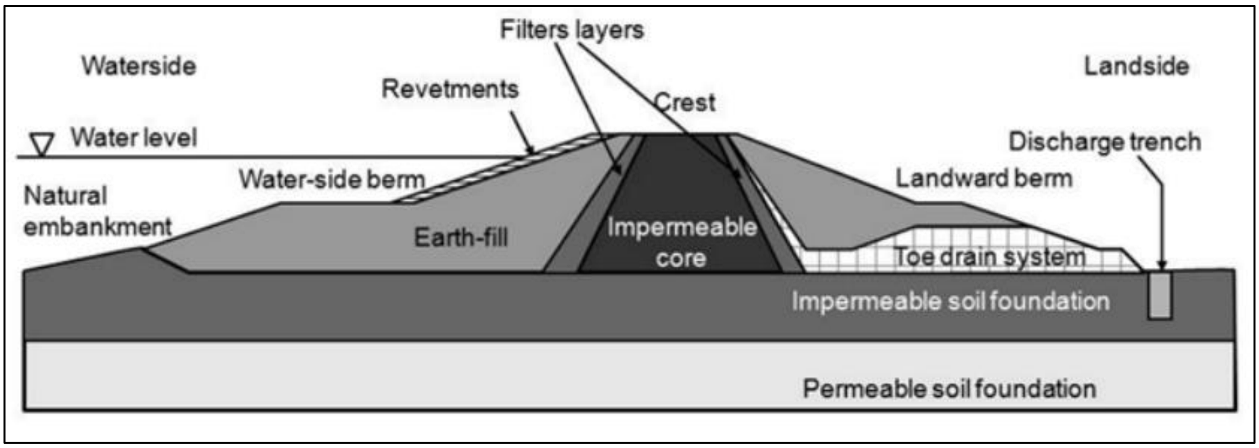

FIGURE 1: General components of a levee (London, 2013).

Levees built on weak foundational material that may not be able to support the levee embankment due to poor shear strength will require a treatment and reconstruction to the foundation (USACE, 2000). Some foundational weaknesses can be attributed to soft and sensitive clay, loose sand, and natural debris (trees, shrubs, branches) deposits. These items are vulnerable to shear failure and may require expensive remediation treatment by excavation to reduce risk. It is important to note that some levees have not been loaded to their design capacity which may create a false sense of security for the level of protection (London, 2013). Understanding the geotechnical properties of a levee is elemental in understanding its effectiveness and reliability. Most all levees are man-made and range in condition from older, poorly maintained levees to engineered embankments that adhere to modern standards and practices. Some levees might come into contact with water very rarely while others control water dynamically over short periods of time. Levees vary from each location in regards to geology, construction history, exploration data, repair history, past performance, and frequency of flooding; it is imperative to perform a thorough investigation before modifications or construction is made on the levee.

Figure 1 is a levee system with many components where each component is an individual function crucial to the effectiveness of the levee itself. The foundation soils beneath the levee are highly variable depending on the local geology and also vary in strengths. Some foundation soils are not optimal for levee construction so they must be considered in the design. A minimum requirement for the foundation soils is that they must safely support the weight of the levee and have impermeability services (USACE, 2012).

The earthfill is a large component to all levees and is usually composed of a local granular material. If conditions are not ideal, earthfill material can be borrowed from an off-site resource. The purpose of the earthfill is to remain stable when water pressure becomes too high and minimize seepage through the levee. If the earthfill cannot withstand the water seepage and becomes permeable, the center impermeable core composed of clay material is added. The impermeable core is always composed of material such as clay as to reduce seepage through the levee.

The levee crest, also known as a crown, is a flat surface whose function differs depending on the needs of the levee. The crest can act as a surface in which water spills out of, such as a spillway, or serves the purpose of another water infiltration protection system. The crest is flat so it may be able to provide access to roadways or maintenance. The crest and revetments are both external items to provide protections against environmental agents that could cause erosion. The revetments are more of an “armor” to deflect any erosive properties, composed of material such as rip-rap or asphalt, etc. revetments can be constructed on both the landside and waterside, both performing functions to reduce external erosion.

A berm is a continuous part on both sides of the levee, typically composed of local earth material. The purpose of a berm is to create balance and stability by putting more weight on each side of the levee. There are several types of berms, and each serves a purpose based on the design of the levee. For example, a levee with a toe drain is detailed as the drainage system in Figure 1, other levees may display other drainage patterns. This example shows the water draining out into the landward side of the levee as a toe drain system into the discharge trench. The drain should have the full capacity to carry out the entirety of the discharge from the foundation area. The purpose of a drainage system is to properly drain the water to control the seepage through the embankment.

Although not shown in Figure 1, an I-wall can be included in a levee system, usually in the middle of the levee. I-walls can be constructed out of concrete or steel sheet piling and can raise the height of the levee. The purpose of an I-wall is to protect one side of the levee, usually the landside, by providing an impermeability barrier, improving the effectiveness.

New Orleans Geology

The purpose of this study is to investigate the use of UAS imagery as a tool for monitoring I-walls and their failure. While the study site is not in the city of New Orleans, the modes of I-wall failure that occurred in New Orleans during Hurricane Katrina will be simulated through construction of a model I-wall at the University of Mississippi Field Station.

New Orleans is located upon a thin deltaic plain above the Atchafalaya Basin where the majority of the sediment is Pleistocene age (Rodgers, 1984). Most of greater New Orleans is characterized by several layers of swamp deposits under the Mississippi River Delta. These materials are very permeable, compressible and commonly contain weak horizons. These horizons often have with thin lenses of flocculated clay that exhibit strain softening. This strain softening causes a significant loss of shear strength that is often compressible (Seed et al., 2008). This soft and swampy sediment deposit is not an optimal foundation for infrastructure.

New Orleans was built in the southernmost part of the Mississippi River system as a river port for the transportation of goods to the people on the Mississippi River system. To reduce the flood risk, the city was built atop a natural levee where the sediment borders each side of the river (Snowden, 1980). As the city was expanding in the 1900s, more land was needed to fit the growing industry and population so wetlands were drained by a “canal-and-pump” system invented by an engineer, Baldwin Wood. Artificial levees were built to protect the drained land from flooding or overtopping. However, the geology of New Orleans is composed of extremely soft sediment and easily compressible soils therefore subsidence became an issue. The battle against flooding and subsidence is a continuous problem between New Orleans and the water surrounding the city.

Originally, the City of New Orleans was built on the higher portions of marshland along the Mississippi River and then further extended to nearby Lake Pontchartrain (Van Heerden, 2006). Marshlands are relatively flat areas with tufts of grass growing in the mud and open water throughout the area. After marshlands were drained, the land beneath was discovered to be peat which is a poor surface to build on. These low-lying, newly drained areas were prone to subsidence. The Mississippi River flood of 1927 exacerbated the problems, leading to the passage of a flood control act in which the Army Corps of Engineers constructed flood control structures along levees to protect areas from floods. During and after Hurricane Katrina in 2006, these levees and floodwalls were breached and overtopped, allowing the water from the Gulf of Mexico, Lake Borgne, and Lake Pontchartrain to flood New Orleans (Comfort, 2006). The levees systematically failed while the winds from the storm moved from the Gulf of Mexico through Lake Borgne, overwhelming the drainage canals with backed up water (USACE, 2000). Hurricane Katrina resulted in over 1600 fatalities and $30 billion in damages and economic losses (Link, 2010).The growth and expansion of the city of New Orleans has only led to more chronic environmental issues directly related to the local geologic conditions (Snowden, 1980).

After the destruction of Hurricane Betsy to New Orleans in 1965, there was a hurricane protection system put in place and the system was not changed until after the effects of Hurricane Katrina (Link, 2010). This outdated hurricane protection system had incomplete floodwall designs and resulted in many legal battles after Hurricane Katrina passed. Considerable efforts have been made to create strong flood control structures in New Orleans. The growth of New Orleans is a continual process to minimize geohazards that may pass through the city.

Subsidence and Sea Level Rise

Large portions of New Orleans are below sea level due to continuous subsidence and sea level rise. The city of New Orleans is built atop soft sands, silts, and clays; subsidence is increasing due to the consolidation and compaction of these materials and soils from local groundwater pumping (USACE, 2000). Ongoing subsidence and sea level rise have combined to create a problematic situation, whereby flood control infrastructure must continually be improved and elevated to provide a consistent level of protection. When major flood control structures (i.e. floodwalls) are constructed, the sediment on the ground is not strong enough to hold the framework properly (USACE, 2000).

The US Army Corps of Engineers anticipate subsidence when planning the design of floodwalls. The planned location of each I-wall is carefully examined for site-specific conditions such as soil type and how sediment might settle according to subsidence (USACE, 2009). For example, I-walls built on soft or weak foundations, the Army Corps Engineers would suggest a lift for a higher elevation allowing the soils to consolidate and increase in shear strength. The added height does affect the environmental footprint of a levee system and aids in the expect of long term settlement.

According to the Louisiana Coastal Area Ecosystem Restoration Study Report (2004), the relative subsidence rates range from 0.5 ft. per century to 1.0 ft. per century throughout coastal southern Louisiana. Combining these values with the eustatic sea level rise of 1.3 ft. per century (IPCC, 2001), the natural subsidence rates range from 1.8-2.3 ft. per century. With these projections, future changes in surge elevation can be estimated. Future design and construction of levees will have to be modeled after this predicted natural subsidence rate. The district of New Orleans regularly assesses these values to periodically revisit levees to see any change or displacement in the I-wall. Any minor movement should be noted after major storms to maintain a structurally sound design.

I-wall Design and Construction

The focus of this research stems from the I-wall failure in New Orleans, I-walls and their failure mechanisms will be analyzed in greater depth. The U.S. Army Corps of Engineers is responsible for the design and construction of floodwalls along the Mississippi River and New

Orleans area. An I-wall is designed to raise the level of flood protection without expanding the footprint of floodwall protection (Duncan et al., 2008). Floodwalls are built when there is not enough land to construct an earthen levee with a good factor of safety at the required level of protection needed. There are many types of floodwalls in place; the bulk of these are I-walls, T-walls, and a lesser known L-wall (US Army Corps of Engineers V-5, 2012).

T-walls are used in place of I-walls when an I-wall cannot reach the specified height safely. I-walls are aptly named for their cross-sectional area takes the shape of the letter “I”. An I-wall is relatively short and is mostly used as a transition unit between the levee and T-wall. An I-wall has a 4 ft. maximum height with an included 6 inches of overbuild; this has historically been added to prevent future subsidence in soft soils (USACE, 2012). An I-wall is typically constructed by driving a steel sheet pile through the center of a levee, to where it penetrates the foundational soil and cuts off the flow of water beneath (Duncan et al., 2008).

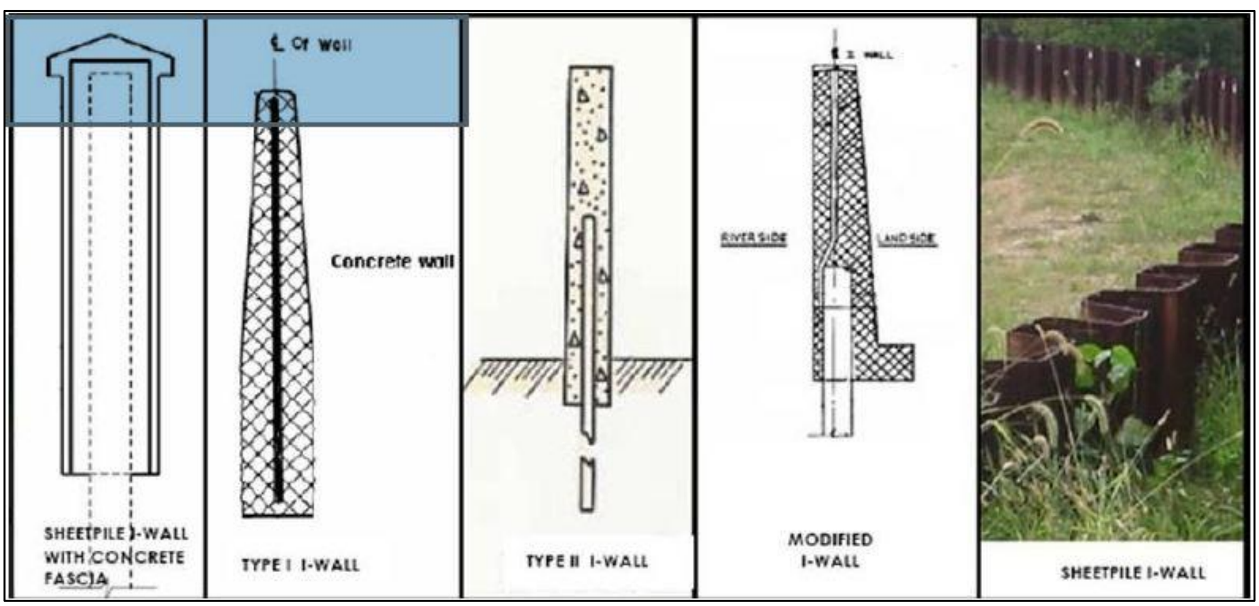

FIGURE 2: Examples of I-walls (USACE, 2009).

The US Army Corps of Engineers employs many of the Type II and Sheetpile I-walls, shown in Figure 2. These two types of I-walls failed during Hurricane Katrina because the exposed side was vulnerable to waves due to overtopping of the I-wall during the peak of the hurricane. Another reason for failure was the erosion formed from storm surge from Hurricane Katrina and therefore creating instability and wall stability issues (Cheuk et al., 2005). Post Hurricane Katrina analysis showed a crack in the concrete at the base of the 17th Street Canal I-wall on the flood side that was deepened due to the hydrostatic load; these I-walls were not designed for the loading conditions presented by Hurricane Katrina. With this increased load, the levee section failed through a combination of instability and then under seepage on the protected side (USACE, 2009). The catastrophe of I-wall failures during Hurricane Katrina resulted in the design and development a manual to provide criteria for stability and seepage analysis (USACE 2012). The analysis detailed in this guide should be used as a reference when assessing any I-wall for up-to-date performance. This guide is used for risk analysis and a dissection of I-wall performance for flood protection.

I-wall Monitoring and Modes of Failure

Floodwalls must be constantly monitored for signs of settlement, departure from vertical and other aging phenomena. There are several failure modes associated with I-walls, but are generally classified into four categories: overtopping, surface erosion, internal erosion (piping), foundation slides (USACE, 2000). Most floodwall failures in New Orleans occurred with erosion due to overtopping and weak soil foundation. Overtopping and erosion were the culprits behind the failures and the soil underneath the levee could not resist the rapid velocity of water flowing. Due to the under seepage, high uplift pressures, and erosion, the foundation proved to be unstable and aided to the levee breaches. Subsequently, there was flooding in the areas that the walls were designed to protect. The U.S. Army Corps of Engineers composed an assessment of the performance of the floodwalls and levees and the cause behind the failures (Ubilla, 2008). Another primary effort that aided in the investigation of the aftermath of Hurricane Katrina, was the Interagency Performance Evaluation Task Force (IPET) (Link, 2010). This group, established by the Chief of Engineers, helped repair and rebuild an updated hurricane protection system. Predicting failure requires a study of both hydraulic and structural features during the critical flooding periods. A levee is built with an ideal resilience to breach during critical flood stages (London, 2013). During Hurricane Katrina, four major levees reached their design limit and failed, allowing the majority of floodwaters to enter the city of New Orleans (Link, 2010).

Overtopping is caused by levees breaching and allowing floodwaters rush through because the height of the water is higher than the levee (Brandon, 2008). When there is significant time to prepare for the flooding, overtopping will not cause significant damage. For example, in the event that a storm is approaching where floodwaters are expected to be high, sandbags are placed atop the levees to temporarily raise the levee to prevent overtopping. Water may flow as under seepage through the levee if the overtopped levee is not protected and reinforced on the landward side. If water flows through a levee that is built on poorly compacted materials, liquefaction may occur and collapse the levee on itself.

In Figure 3a, the main cause of breach was due to a split in the I-wall that introduced high forces down the face of the sheet pile, causing a foundational failure in the area of 17th Street Canal. This area is known for having a weak clay foundation – that results in foundation instability in the flood control system. As water was rising, it seeped through the gap that lead to translational failure. This resulted in lateral movement of the floodwall along a shear plane in the weak clay foundation below peat. Levee geometry, floodwall depth of penetration, and underlying soil profile were critical to the performance of the system under flood loading

(Duncan et al., 2008). An important finding in the IPET investigation of Hurricane Katrina was that these gaps, caused by cracks in the concrete, reduced the stability of I-walls (Brandon, 2008). Gap formation was found to be a principal factor behind the failures and breaches. Gaps are likely to form when soil materials on the protected side are soft and easily compressible. The variability of the softness or stiffness of soil is difficult to predict, so it is hard to estimate the exact time of an I-wall failure. In Figure 3b, the I-wall has sand beneath the levee that creates a hydraulic connection between the water in the canal and the sand. This creates an environment where erosion and movement is more likely to occur and increases uplift pressures, reducing the stability (Seed et al., 2008).

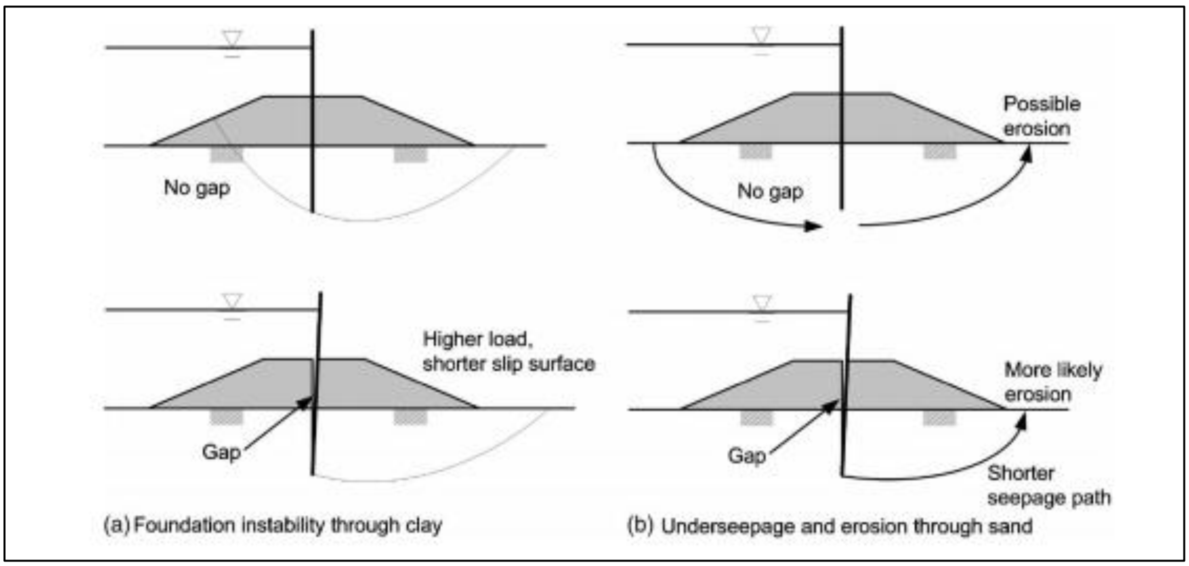

FIGURE 3a-b: Schematic representation of I-wall failures. (a) Foundation instability through clay and (b) Underseepage and erosion through sand. (Duncan et al., 2008).

In technical terms, overtopping does not refer to a failure so much as a function to which the factor of safety and level of protection decreased. The Army Corps of Engineers states floodwalls that overtopped and failed have achieved their designed function. The water was held up to a certain elevation at the top of the wall, but significant water impact created flooding. Floodwalls may fail when water overtops the crest of the levee, this can be prevented by creating a flood resilient wall to reduce the risk of overtopping. Most floodwalls in New Orleans failed due to overtopping but some failed because water seeped through the bottom of the foundation causing the I-wall to shift resulting in a breach.

Floodwalls often reinforced with rocks and/or concrete to prevent failure. Depending on the surrounding strength of the soils, failures can happen quickly or over time, as erosion takes place. The soil should have a high factor of erosion resistance so to avoid failure by overtopping. Newer walls have been designed with scour protection on the landside between the levee embankment and wall section (USACE, 2005). Scour refers to the removal of hydrodynamic forces of sediment and materials in the area near floodwalls. Scour is a more specific form of erosion.

Surface erosion is usually caused by action of wind, water, and/or waves. Erosion can be worsened by pre-existing damage to levee. Significant vegetative growth such as trees on levees can increase the risk of levee failure; trees saturated with water become unstable within the soil of the levee. When a tree falls and pulls out the root system, it can remove saturated soil, producing a shallow hole. This hole can erode quickly to result in a levee breach. Large trees near the floodwalls have the possibility to topple over during a major storm and cause damage to an adjacent wall. Other vegetation on either side of the wall can potentially have adverse effects to alter the stability in a negative way. The USACE (2009) defines a “safe distance” from the foundation of the wall to any vegetation to be 15 ft. This value is given as a safety precaution, where vegetation within this 15 ft. may be harmful for the stability of the wall and could potentially cause failure. All walls should be evaluated independently for different soil and vegetation types behave uniquely.

Foundation failure can happen gradual or sudden, on surface or subsurface and can often be accompanied by sand boils. Boils signal a condition of instability which may lead to erosion of the levee toe or foundation. Resulting in sinking of the levee into liquefied foundation below.

FIGURE 4: 17th Street canal breach caused by stability failure. Breach circled in red. (Duncan et al., 2008).

The USACE (2009) has measures in place to reduce the prospect of a levee failure. Risk analyses are routinely performed on each levee which includes inspections for maintenance and risk reduction. Depending on the area the levee is in, more specific actions are in place that can lower the probability of a levee failure based on geotechnical and environmental factors. An example of a more specific factor is to reducing the level of water from river channels by removing debris in the water. This can directly impact the levee by reducing pressure on the levee. Another example would be to install drainage structures to collect and control seepage (Seed, 2009) and increase the stability of the levee.

Structure from Motion and Unmanned Aerial Systems

Combining geospatial technologies such as UAS and SfM photogrammetric methods can revolutionize mapping for scientists, engineers, surveyors, and many other sectors (Madden et al., 2015). Photogrammetry is the science of gathering spatial data and geometrically derived information from photographs (Lillesand et al., 2004). Traditional, photogrammetric methods use overlapping images to align points within a scene, which required hours of manual matching and alignment (Ullman, 1979). The camera locations and optics of the camera were necessary knowledge to proceed with this type of traditional photogrammetry. SfM can solve for these issues by gathering information about internal parameters and exterior locations of the camera and angles. The University NAVSTAR Consortium (UNAVCO) defines SfM as the photogrammetric method for creating 3D models of a particular area of interest from overlapping 2D imagery taken from various locations and orientations to reconstruct a final scene (Shervais, 2015). This automated process identifies similar features in each image while gathering external camera parameters and uses 3D-based algorithms to produce models such as point clouds and DEMs with accuracy similar to TLS (James and Robson, 2012). TLS is a ground-based LiDAR method for 3D datasets at a sub-centimeter resolution (UNAVCO, 2017). Both TLS and SfM methods use a feature detection system that has a batch block adjustment is made to match the XYZ location of each feature to create a sparse cloud using the scale invariant feature transform (SIFT) (Lowe, 2004). SIFT can be used for image stitching, 3D modeling, and object recognition. Any SfM algorithm can gather information about depth just by data from the motion of the camera. Scenes are then constructed by camera positons and orientations plus topography (Shervais, 2015).

There are many advantages of SfM compared to LiDAR methods. These include low-cost and competitive pricing, any recreational user can purchase some form of a UAS and an open source photogrammetric software to process their images. Another benefit includes ease of use, the only required equipment is a camera mounted on a UAS and a computer capable of processing data. A disadvantage that may arise with UAS versus terrestrial laser scanning is the accuracy and precision that a UAS may not be able to achieve. Recent findings show modern UAS capable of reaching a millimeter scale for a slightly higher cost (Choung, 2014). In this study, the use of UAS for geometry and point cloud creation of a levee is appropriate and has the possibility to improve levee monitoring. Both methods are able to obtain high precision. With small to medium sized areas with limited vegetation, the combined use of UAS and the photogrammetric methods of SfM are a potential system for flood wall monitoring.

Aerial photography using UAS is becoming a common and economical form of remote sensing. Some advantages of aerial photogrammetry over other photographic systems include improved vantage points, permanent recording, broadened spectral sensitivity and increased spatial resolution (Lillesand et al., 2004). UAS are advantageous when it comes to an area of interest with low accessibility, such as levees of flood control structures. With UAS, it is easier to see the “big picture” of the area of interest because of the bird’s eye view allowing the user to collect larger spatial areas (Ridolfi et al., 2017). Improved vantage points from different camera angles on the UAS can help the user map all observable features in 3D during one flight acquisition. A single flight acquisition could capture numerous photos and send them out to many users for analysis and comparison. Another advantage of aerial photography is a broadened spectral sensitivity where invisible UV and near infrared energy can be collected and output as a visible image in a display system or photograph. Lastly, an increased spatial resolution allows the user to record more spatial data when the image is magnified. The data on the image can be geometrically corrected with the right ground control data as a reference

CHAPTER III

METHODS

To use time and materials more efficiently in the field, it was deemed paramount to use a structured approach to design a model. Using a structured workflow, uncontrolled variables can be mitigated, uniformity can be produced, and the operation can be repeated for multiple flights. A workflow has been created for the scope of this project as to maintain consistency. Each of the categories listed in Figure 5 have a specific purpose in identifying movement in a model I-wall and employ principles of SfM, UAS modeling applications, and I-wall monitoring.

FIGURE 5: General overview of methods used.

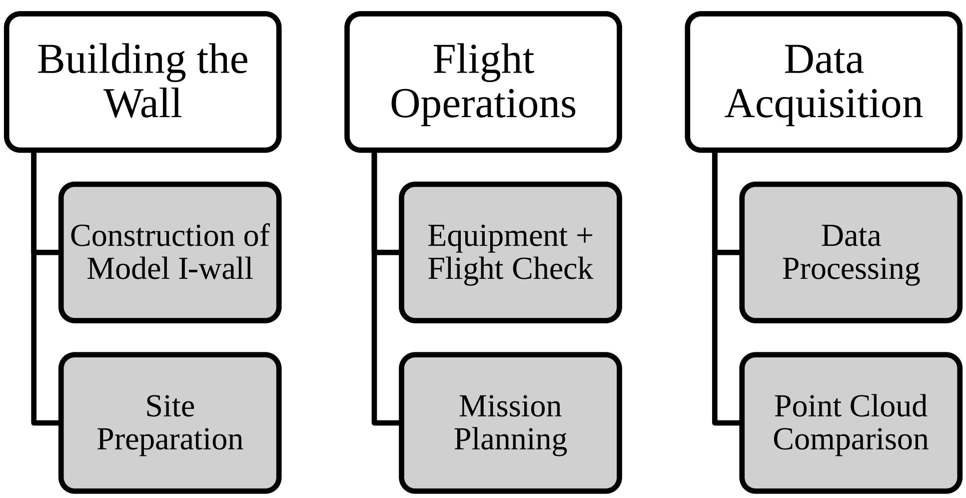

Construction of Model I-wall

The USACE provides a manual with specific measurements of I-walls and the mock I-wall constructed was designed based on these specifications (USACE, 2000). Using these measurements, a scaled-down model of a typical I-wall was constructed with proportionate sizes. The design for the mock I-wall is outlined in Figure 6; the angle that the wall will be manually tilted at is displayed by a red θ. The two holes dug in the ground to support the I-wall were filled in with compacted backfill and pressure treated lumber wood. Supporting the wall, the two wooden square panels were used to support the wall for foundational balance and allowed the wall to be manually shifted to alter the angle. The panel frame was constructed to simulate a typical I-wall. A few modifications were made throughout the project to improve the operations so the UAS would be able to more clearly see the top of the wall for further processing. These modifications include adhering colored duct tape to the face and backside of the mock I-wall for clarity and contrast during processing. Another modification included flying over the wall in a more structured flight path approach so the area can be captured more accurately.

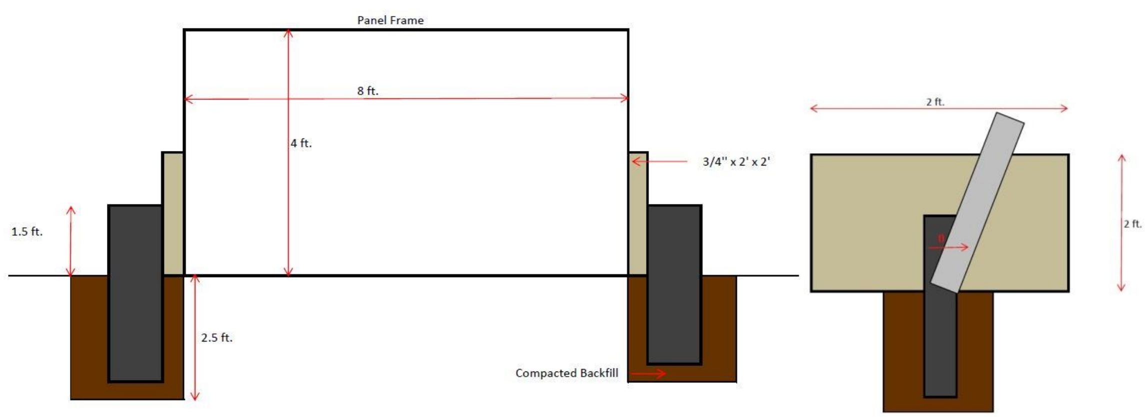

FIGURE 6: Mock I-wall constructed at University of Mississippi Field Station. The figure is not to scale.

In Figure 7b, the image shows a front view of the mock I-wall. Two holes were dug, as demonstrated in 8a. The holes were dug 2.5 feet below the surface, this is to resist any movement caused by natural or environmental factors that could affect the stability of the mock I-wall. The wall framework was covered with white corrugated plastic board that can be removed if necessary (Figure 7c). Figure 7d shows the UAS on one GCP, ready to begin a flight acquisition. For consistency, the UAS took off in the same position for each flight.

FIGURE 7a-d: Construction of mock I-wall (a) Hole dug for posts, (b) Front view of mock I-wall, (c) Back view of mock I-wall, (d) View of GCP with I-wall in distance.

Site Preparation

The University of Mississippi Field Station (UMFS) was chosen as the site for this project because of its favorable conditions. The field station (Figure 8) is in a secure location secured by a surrounding gate and is not near any airports, therefore no airspace restrictions. The UMFS is mainly used for biological research so the amount of people present at one time is minimal. This is a public research area but there is never a concern for a collision with the overhead flying UAS. The area within the UMFS was chosen for its uninhabited and semi-vacated land, there are no trees in the direct area of research; the trees surrounding the study area provide a physical barrier to other outside elements. This location has a wide variety of land cover, the contrast of the green grass the white mock I-wall provided an excellent distinction in points when processing. The exact location was chosen because it is far enough away from the access road to avoid any oncoming vehicles and near the shed for an access to nearby tools.

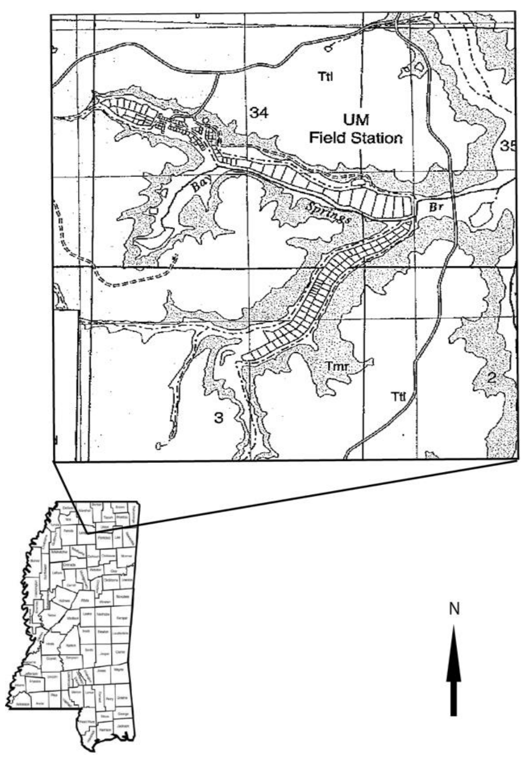

FIGURE 8: Location of the University of Mississippi Field Station (Okoye, 2013).

Other conditions need to be met before flight such as weather and light conditions. Dark shadows and illuminations can hamper the imagery alignment process. Shadows will have an impact on the performance of the algorithm since it is searching for similar features. Performing these checks before each flight will reduce the chance of small errors to occur and increase consistency.

To begin with correct site preparation, GCPs must be laid out in proper placement. With the ultimate goal of a point cloud for comparison , the ground control points create a reference for this model to be positioned within in a coordinate system, to increase the accuracy. GCPs can be any color or shape; they must be at least large, marked targets on the ground. A GCP with contrasting colors is best. A minimum of four is necessary and should be placed strategically around the study of interest, most likely on the boundaries of the study area (Ridolfi et al., 2017). When using GCPs, the global position satellite (GPS) coordinates need to be determined for each control point. To determine the exact GPS coordinate for each point, an EMLID Reach RS+ real time kinematic (RTK) Global Navigation Satellite System (GNSS) receiver was used, shown in Figures 9 a, b, c. RTK GPS is a technique used by applying satellite navigation to enhance the precision of positional data derived from GNSS satellites. The time it takes for the signal to travel from satellite to receiver is how the user measures the distance and therefore position of the object.

For recreational users, using a relative model without GCPs is feasible; distances can be measured albeit without great accuracy (Ridolfi et al., 2017). For professional UAS survey users, the use of GCPs greatly increases the global accuracy of maps. The exact orientation of objects defines the accuracy of the research and allows the model to fit in a geodetic coordinate system. To ensure total accuracy, the GCPs help relate the latitude and longitude of that point to the GPS coordinates (Smith, 2001). The GPS base station will be left to dwell on the center of the GCP for approximately 20 minutes to further correct any ephemeral errors. The time required to detect the presence of satellites is referred to as dwell time. The dwell time is based on a combination of a correlation of received signal and a reference signal (Cheuk, 2005).The longer the RTK GPS dwells over the GCP, the more likely the presence of a satellite signal can be tested for a certain combination of parameters therefore increase accuracy. The dwell time shows the user if an object has not left a defined location (Smith, 2001).

Once the GPS receiver is affixed to the tripod, the tripod is then balanced and plumbed vertical to the ground. Each GCP station is set to dwell for about 20 minutes. Using the ReachView app, the correction input, solution output, and update the time configured. Figure 9 displays the applications screens when powered on. A standard Phantom 4 Pro UAS has an internal accuracy of +/- 1-5 meters. Using GCPs with a survey grade RTK GPS system, the values of accuracy increase ten-fold (Martínez-Espejo, 2017). To obtain relative accuracy, GCPs are not necessary but since this study requires precision level measurements, absolute accuracy is necessary.

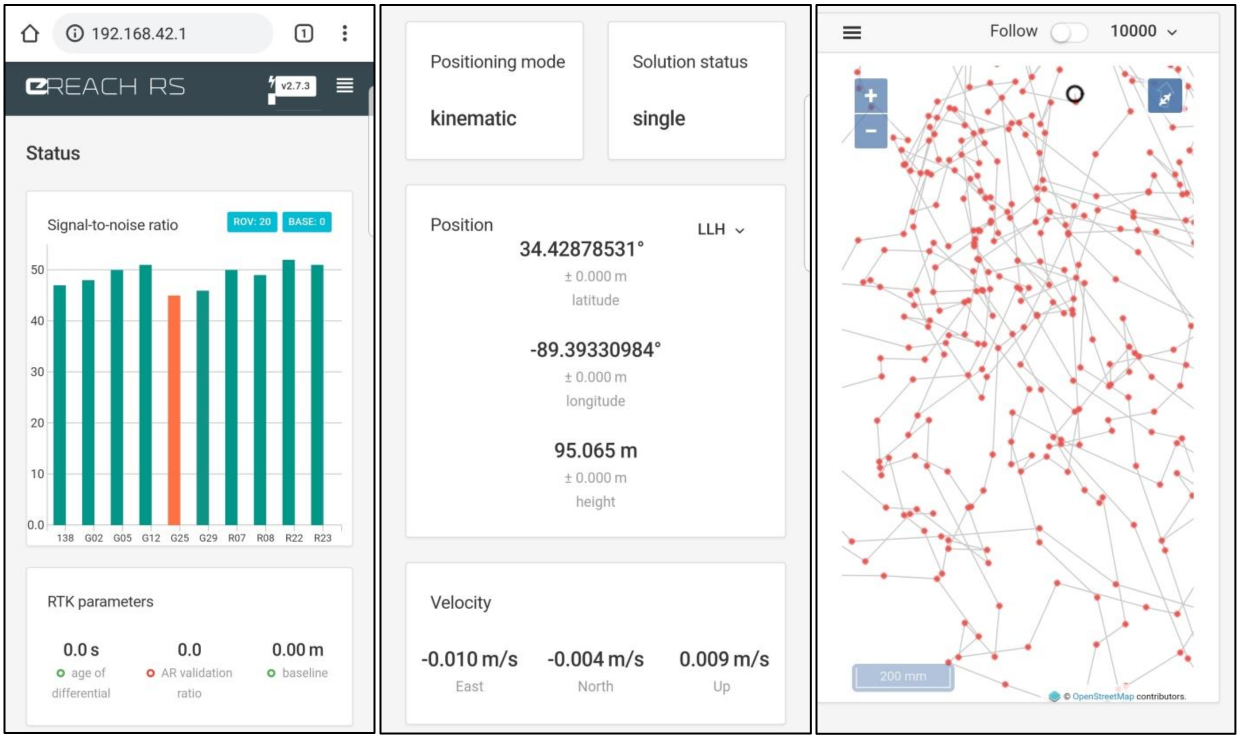

FIGURE 9a-c: EMLID Reach RS+ RTK screens (a) SNR, (b) Location page, (c) Map. This figure is not to scale.

For this study, GCPs were created out of corrugated white board and black tape created a symbol '+' for known middle point clarity. The white color is a good contrast to the green vegetation surrounding it. The shape and style of this control point was chosen for easy identification purposes, this can be shown in Figure 10a.

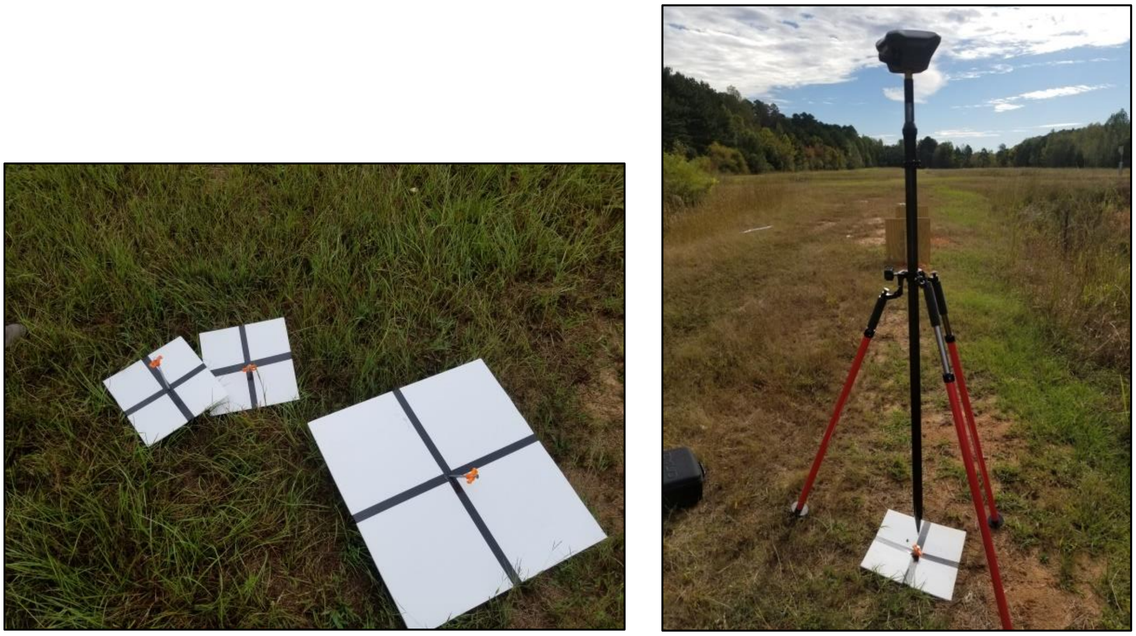

FIGURE 10a-b: GCPs and RTK equipment at UMFS (a) GCPs, (b) EMLID RS+RTK in field station.

Once the GPS coordinates are recorded of each GCP, they can be entered into a tabular format for input into Agisoft. The Z-values will be omitted because the ground is relatively level and will not impact the accuracy of the data collection. Coordinates of the first three GCPs are shown below in Table 1.

TABLE 1: Coordinates of each GCP. Datum: WGS84.

GCP Label #	Latitude	Longitude
Point 1	34.42878446	-89.39330676
Point 2	34.42878146	-89.39320209
Point 3	34.42874129	-89.39315423

Equipment Check

The Phantom 4 Pro by DJI was used in this study. It is an entry-level professional drone with obstacle avoidance. While used by many recreational hobbyists, this UAS is dynamic enough where it can also be implemented in professional research studies. The titanium alloy and magnesium alloy body of the UAS provides a lightweight yet rigid system to ensure stability on each flight. All aircraft specifications from the DJI website are detailed in Table 2.

The onboard camera uses a 1-inch 20 megapixel CMOS sensor that also eliminates shutter distortion when moving at high velocities. The camera was not switched out for a different one to eliminate error from making adjustments to the UAS. The same camera is used for all acquisitions to reduce errors caused by different equipment mounting. The weight is evenly distributed with the current onboard sensor so no corrections are needed to account for camera placement adjustments.

A favorable advantage to this UAS over other options is the five-direction obstacle sensing where two high resolution stereo vision sensors are placed in the front and two in the back. This creates a four-directional obstacle avoidance and a five directional obstacle sense. According to the Phantom 4 Pro manual, the sensors in the UAS can detect an object as far as 40 feet away and then plan a route to avoid collision in a direction it chooses.

TABLE 2: Aircraft specifications.

Aircraft	**Specifications**
Weight	1388 g (without additional external sensors)
Satellite Positioning Systems	GPS/GLONASS
Sensor	1" CMOS, Effective pixels: 20M
Lens	FOV 84 deg.
ISO Range	100-2300 (auto)
Maximum Flight Time	~30 minutes
Rising Speed	5 m/s
Descent Speed	3 m/s

The camera was automatically set to a shutter priority of 1/1200 to reduce any motion imagery and the aperture was set to a focal length of 3.5. To maximize the values of the camera settings, images were set to capture every 1.5 second automatically. Images can be taken manually, but to improve consistency, images were at regular intervals.

The MicaSense RedEdge-M multispectral camera kit is used in addition to the UAS to more clearly outline the edge of a wall. This can be attached to the UAS or used separately by manually holding it over the object in question and capturing the images. The RedEdge-M simultaneously captures 5 spectral bands. Red, green, blue, NIR, and red edge M band (usually for agriculture or environmental purposes). There is a downwelling light sensor that directly connects to the RedEdge-M camera which can measure how much light enters the camera and how it affects each of the five bands. The camera is powered by the devices' Wi-Fi that can be used in conjunction with any Wi-Fi-capable platform to preview live streaming of images.

A multispectral method is considered because this may be able to aid in capturing image data within specific wavelengths, meaning this could create a contrast in the point cloud to define the clear edge of a wall. Using a multispectral method, the UAS can only see reflected energy from object in the three channels that are red, green, and blue. Employing a multispectral sensor, visible and infrared radiations can be viewed. A multispectral lens can be added to the camera system onboard the UAS and can analyze richer spectral data. A multispectral imaging system can aid this research by noting extremely small changes through contrast with infrared tape, which is necessary for detecting minute changes in the modeled I-wall. When determining temporal resolution, flight time and battery life needs to be considered. The observation of a constantly changing task, such as a levee failure, is best detected with UAS technology (Brauneck et al., 2016).

This multispectral camera also works best when there is a contrast available – such as the mock I-wall against the vegetation. The contrast allows the resulting point cloud to adjust the points accordingly to clearly define the edge of the white mock I-wall and the lush, green vegetation. NIR is sensitive to chlorophyll. When chlorophyll is vigorous and active, it gives you a larger response to NIR. Chlorophyll is directly related to health and vigor of a plant so mounting the RedEdge-M onto a UAS can allow you to easily and economically measure specific characteristics of vegetation. Although the RedEdge-M multispectral camera was not used directly in this study, it is important to note that it can be used an as addition to the UAS to help define edges of the wall. An experiment was run manually by physically holding the equipment to capture images above a wall with a piece of reflective tape on the edge. The RedEdge-M apparatus covers the obstacle sensor on the UAS and prohibits the use of this detector when in flight. This is a safety concern when flying overhead near any vegetation or forestry. This type of equipment can be added on for future research but cannot be applied to the current UAS for a safety concern.

Flight Check

There is a standard operating procedure and certain safety measures that need to be taken into account for when preparing for a flight. This flight operation is operating under the Federal Aviation Administration (FAA) Section 107 rules. The FAA provides standards and regulations flying that should be acknowledged before flight; these can be found online on www.faa.gov. While it is not necessary to obtain a license for recreational UAS usage, it is good practice to have one when flying often.

The University of Mississippi Department of Geology and Geological Engineering coupled with the Geodata Analysis Laboratory (GDAL) have a UAS Flight Planning and Operations guidebook for students and faculty to reference when obtaining use of the UAS in preparation for flight. Outlined in this guidebook is a pre-flight checklist, a take-off policy, and a landing policy. This guidebook is created in hopes of a safer environment to ensure proper recreational UAS use.

1. Pre-flight checklist
    a. Request permission for flight if location is over Restricted Areas.
    b. Check Zone map with DJI's Geospatial Environment Online (GEO) where the system delineates restricted zones, or where it is safe to fly.
        i. https://www.dji.com/flysafe
        ii. Allows you to check laws and regulations of the specific area
    c. Establish open area for flight with no obstacles including people, moving vehicles, tall vegetation, or power lines.
    d. Check controller for latest firmware update
        i. UAS may not begin flight without proper updates
    e. Confirm environmental variables are within a safe range
2. Pre-flight UAS component check
    a. Check body of UAS to ensure no deficiencies or blemishes that would cause structural weaknesses
    b. Confirm all connectors and wires are present for controller
    c. Rightly fasten propellers
    d. Payload check
        i. If MicaSense RedEdge M is attached, secure and fasten equipment properly

Mission Planning

Mission planning applies both principles of photogrammetry and SfM. Whether a pre-flight plan was created or simple random image capturing system was used, images needed to be shot from many different angles and rotations. One variable that can be controlled is the wall which is manually tilted so displacement can be noted in processing and analyzing the data. Another variable that is part of the mission planning is the height at which the UAS will be flown, and the angle of incidence to capture images. Having a differing angle of incidence provides advantages in capturing images; the UAS is allowed to investigate further aspects of the area with a different angle. These variables are detailed in Table 3 from a preliminary flight acquisition on 08 November 2018. This flight acquisition was repeated 22 March 2019 using updated parameters and methods, developed from the preliminary data acquisition. Planning these flight paths and characteristics are critical to determine any type of movement or displacement within the point cloud.

TABLE 3: Preliminary data acquisition from flights performed.

Flight	Look Angle	Height (m)	Overlap (Sidelap/Frontlap)	Wall Angle
1	Nadir	15	60%/80%	90°
2	45°	15	60%/80%	90°
3	Nadir	30	60%/80%	90°
4	45°	30	60%/80%	90°
5	Nadir	15	60%/80%	35°
6	45°	15	60%/80%	35°
7	Nadir	30	60%/80%	35°
8	45°	30	60%/80%	35°

Mission planning is the configuration utility for UAS and helps setup optimum performance. With any open-source application, appropriate telemetry can be used to assess the size of the area, avoid any obstacles that may arise, monitor vehicles status in operation and host a flight plan with the correct parameters. Carefully combining all of these conditions provided assurance that all objectives will be met during each flight.

When planning a flight, the angle of the sun needs to be taken into account so the intensity of shadows can be reduced. An overcast day is an optimal condition, clouds act in place as a light diffuser (Brauneck, 2016). Overcast reduces the presence of shadows and glare from reflective surfaces. Although weather conditions can never be predicted, favorable parameters will result in the most optimal 3D model. If a user is planning on flying for more than 30 minutes per flight in a day, it is best to complete the acquisition over the course of a few days. The shadows cast from solar procession affect the resulting point cloud and is consistency is needed, its best to fly at the same time during different days (Smith et al., 2001).

The mission planning software used was Pix4D, a free application for a cloud software platform for commercial or recreational UAS use. This utility was straight forward to automate the flight with combined data capture with high quality interactive maps. Pix4D is compatible with several of DJI’s latest UAS and is fully capable of running on an Android system and iOS system. Although Agisoft is used for this study, image processing and analysis is available on the website where the user can upload imagery straight from the UAS’s SD card and ground control points can be input and processed.

Pix4D defines a good map as having 99% coverage of the area of interest, high data quality (focused cameras), sufficient overlap (frontlap and sidelap), and homogenous imagery. In a predetermined mathematical algorithm (SIFT), all features identified in the images will match and align with each other. Settings can be manually adjusted within the Pix4D application. The input data to generate a rigorous 3D model needs to be processed using ultra-high settings for the best accuracy. Flying higher gives the camera lens more area to cover in a single image (Brauneck, 2016). At a higher elevation, the UAS can capture more images with multiple common features in the stitching and alignment process. This is more beneficial when an area displays consistent imagery, such as the UMFS where it is mostly vegetative.

During the second flight acquisition on 22 March 2019, each flight had a set area for a flight path using Pix4D. To gain better coverage of the study area, the UAS flew over the area in a specified grid format and then repeated a similar grid at a different angle. This enables the UAS to gather different angles of the object of interest for better 3D reconstruction. The angle of the camera does not change. Images were captured at a specified interval, every 2 seconds. The speed of the UAS is not an independent variable because it changes based on the input variables. For example, the overlap chosen was 90%, the area measured to be about 39 m x 26 m, wind speed was very low, and the altitude was 30 m. Based on these selected variables, speed will be a reflection on how clear the images are. The actual parameters used for the 22 March 2019 flight is shown in Table 4.

TABLE 4: Second flight acquisition parameters from 22 March 2019.

Flight	Look Angle	Height (m)	Overlap	Wall Angle	GSD (cm/px)
1a	Nadir	30	90%/90%	90°	0.83
2a	70°	30	90%/90%	90°	0.87
3a	70°	15	90%/90%	90°	0.44
4a	70°	30	90%/90%	90°	0.87

Different mobile applications for mission planning are available for use including Drone Deploy, Pix4D, or any open source platform such as Mission Planner. Many intuitive flight apps have been created in response to the growing community of UAS users. The two market leaders in intuitive applications are Pix4D and Drone Deploy (Fraser et al., 2018); Pix4D is the application used for this study. Pix4D is an automated mapping software targeted towards recreational users and pilots; the user captures images then creates maps and 3D models then explores and analyzes the maps. This application allows the user to explore the finished map on any device where it can create ortho-rectified mosaic, DEM, and 3D models. The applications are all built from a cloud-based software where it automates the flight and easily captures aerial data.

A general rule of photogrammetry with aerial acquisitions claims more overlap can aid in the alignment process where features can more readily be matched to each other. Also, with a larger ground sampling distance (GSD), the targets are easier to mosaic. In this context, ground sampling distance is referred to the distance between two pixel centers measured on the ground (Lillesand et al., 2014). GSD may differ with the same height due to the elevation differences in the terrain and the camera angle. There are also camera specifications that can affect the GSD, such as the camera resolution which can determine the amount of pixels the sensor can detect. A higher camera resolution can result in a greater GSD. An example calculation of GSD can be provided by Pix4D in Table 5. The sensor width, focal length, variable flight height, and image width/height is entered and the calculations provide the quantitative number for the ground sampling distance. Smaller lenses produce more distortion and longer lenses, due to the lens curvature. Therefore, images captured with smaller lenses cover larger areas compared to longer lenses. GSD is very important in aerial surveys because it allows the user to assess the distance of one point to another, in pixels, based on images captured by the UAS. Absolute measurement accuracy relies on GSD, and lower GSD values give more precise measurements. Most mission planning software's automatically calculate the GSD when the size of the area is determine, but knowing how these numbers are quantified allows the user to understand what resolution is needed for an area.

TABLE 5: Ground sampling distance calculations for Phantom 4 Pro (Pix4D).

S_w	13.2	Sensor width of the camera (millimeters)
F_R	8.8	Focal length of the camera (millimeters)
H	30	Flight height (meters)
imW	5472	Image width (pixels)
imH	3648	Image height (pixels)
GSD	**0.82**	**Ground Sampling Distance (centimeters/pixel)**
D_w	45	Width of single image footprint on the ground (meters)
D_H	30	Height of single image footprint on the ground (meters)

Both side overlap (sidelap) and front overlap (frontlap) are equally important and can be manually adjusted in the Pix4D application. Flying higher altitudes can allow a higher frontlap percentage. Figure 11 demonstrates the amount of overlap coverage when the percentage is increased. Although a greater overlap percentage is ideal, most UAS flights do not cover a large area. A higher percentage requires a longer, slower flight therefore more battery use that may shorten the duration of flight. Images captured at a constant rate with high overlap at a rapid pace can be subject to motion blur. Motion blur can be caused by a fast moving UAS coupled with slow shutter speed, this can easily be fixed by moving the UAS at a slower speed.

Bemis and others (2014) suggest oblique imagery can be used to amplify imagery taken at a uniform elevation. The angle of incidence should be limited to 10-20 degrees from vertical because a large angle may decrease accuracy when processing. These additions were taken into account for the second flight acquisition and flight variables were changed.

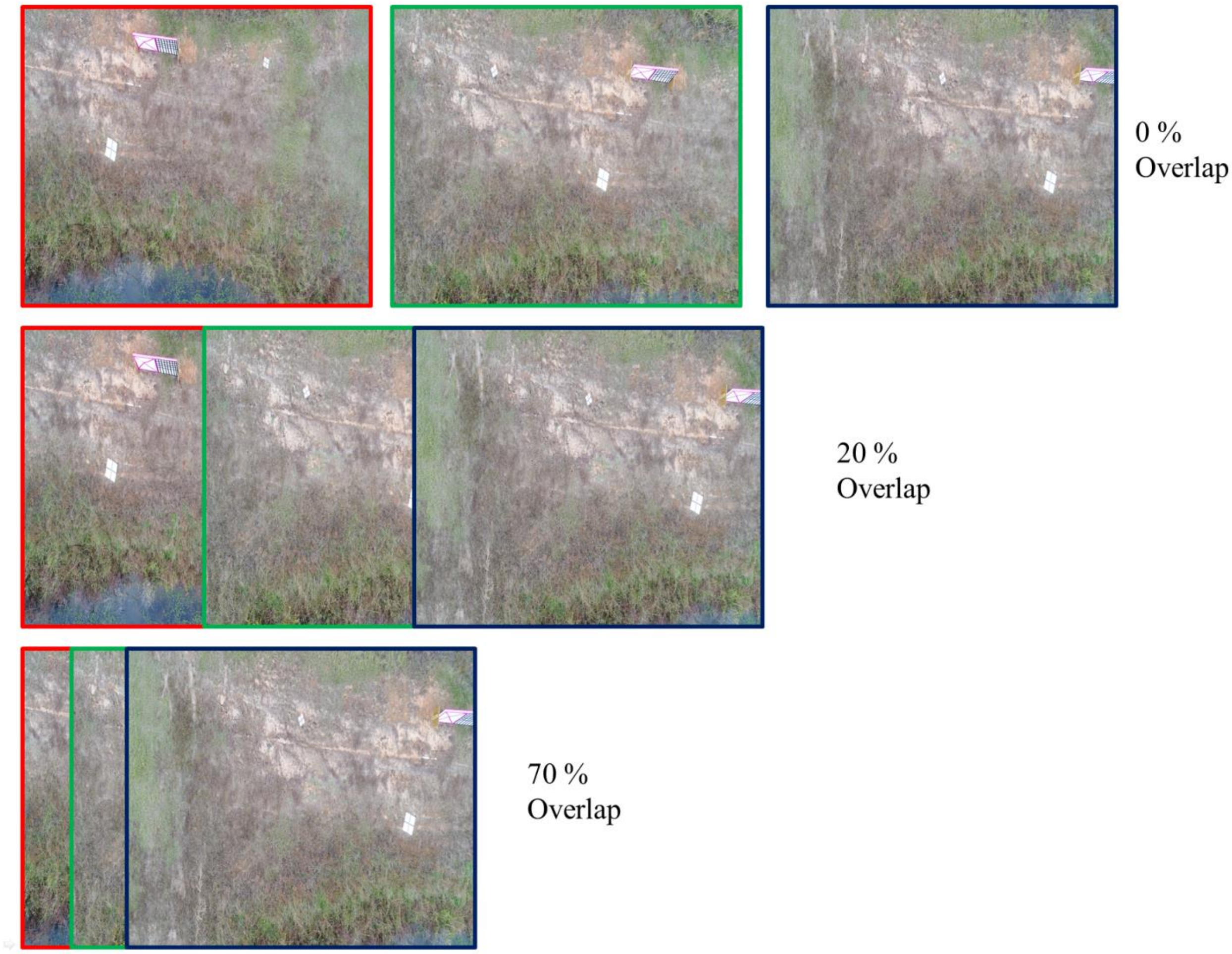

FIGURE 11: Different forms of overlap.

An important note for generating a 3D model with multiple images – is that the images will need to contain a small angle of incidence. An angle of incidence is defined as a measure of deviations from "straight on" (Fujita et al., 2015). When images are only taken nadir, this creates a low depth perception for the computer algorithm to pick up and process. Capturing images solely in nadir may lead to errors in the data processing phase with the point cloud will have a layover effect where the object in question will seem distorted or elongated. Having a combination of nadir and oblique images is best for capturing the full scope of an object and for 3D modeling. The combination of camera angles will capture small areas that nadir would not be able to see.

Data Processing

The data processing category relies on contributions made by previous UAS hobbyists and researchers (Aicardi et al., 2016). With the advent of new technology and faster, more adaptive software, Agisoft Photoscan has been created for professional use and also recreational use. The vast array of applications using Agisoft to create point clouds and 3D models is growing and is important to note as the onset of geo-hazard mitigation is progressing into aerial photogrammetry as opposed to traditional terrestrial methods (Madden et al., 2015). While some may argue traditional photogrammetry methods have more superior point cloud accuracy, UAS-derived point clouds are easier to acquire and at the same accuracy as TLS (Smith et al., 2001).

For the bulk of the data processing phase, Agisoft, proprietary software was used. Agisoft Photoscan is the primary software used for commercial and recreational users in the geosciences. Agisoft does require a fee for the license but then the user is able to export DEMs, place GCPs, and make georeferenced measurements (Verhoeven, 2011). The resulting 3D model from Agisoft is built from the images with telemetry acquired with the UAS during flight acquisitions. There are other free software's that are open sourced and may have a more complex workflow due to the lack of a Graphical User Interface (GUI).

The photos that were input into Agisoft were free of blurriness, collected at a sufficient resolution, and had adequate lighting. If the image input is blurry, the software may not recognize the tie points and will reject the photo rendering it null or making the model skewed.

Tie points are matches between key points detected on two or more images that can be linked to form 3D relative positioning. In Agisoft, if the tie points become outliers, this means the points are filtered out because they are imprecise therefore disabled. Agisoft automatically finds tie points and estimates intrinsic camera parameters during photo alignment. However, the accuracy may be affected by different factors, such as overlap and mismatched features from neighboring photos (Agisoft, 2014). Agisoft uses photogrammetry and Structure from Motion principles. It compares and references points with neighboring images and if the resolution is not appropriate for the desired scale, the quality and accuracy of the final model will be altered. Lastly, adequate lighting is regarded as high importance in the data processing phase because heavy shadows or dim lighting (dusk, dawn), will affect the parameters of the final model thus influence the later comparison of all the chunks, or each flight, with their separate variables. Although unpredictable, weather conditions should be optimal and meet the users' expectations to ensure the utmost accuracy and clarity of images. Poor image input influences the alignment; Agisoft automatically estimates quality and are recommended to be removed. Figure 12 lays out a workflow system to establish an efficient productivity roadmap. The procedure used is detailed in the figure below.

Agisoft operates under the principles of traditional photogrammetry, using defined features capture in multiple images from different vantage points to generate a 3D model. This study emphasizes the use of aerial photogrammetry collected by UAS technique and procedures.

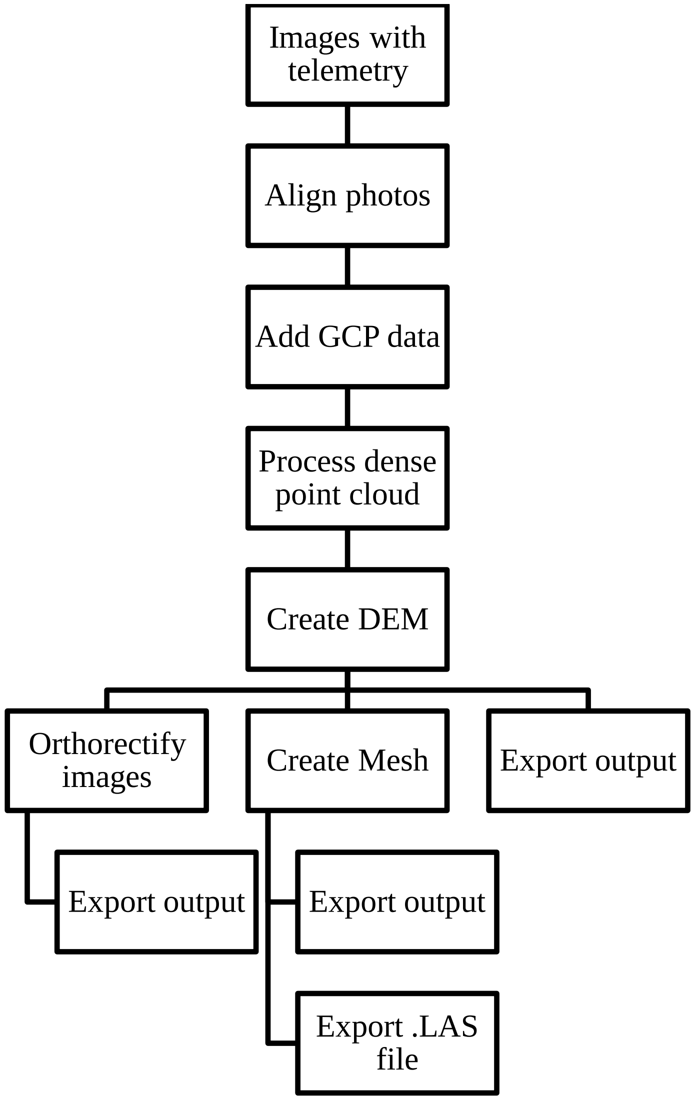

FIGURE 12: General plan of the data processing stage using Agisoft.

Before beginning a new project in Agisoft, certain settings should be adjusted to fit the user's needs. In the graphics processing unit (GPU) tab, all GPU devices detected by Agisoft should be configured to significantly improve processing speeds, shown in Table 6. Agisoft takes advantage of GPU processing power that can allow the software to process images at an accelerated pace. This is done by GPU-accelerated computing (Rossi, 2017) where the functions that require compute-intensive sections are forwarded to the GPU and the remaining sections are executed through the CPU. Parallel computing using the GPU is dividing a large problem into various smaller tasks that will operate in unity to form a solution. When parallel computing, the executions of processes are carried out at the same time. A GPU typically has hundreds of small cores that operate collectively using parallel architecture to display high performance. This uses the ability of parallel processing where the application has faster speeds because of the simultaneous processing of the GPUs. When processing large amounts of data, like the ones used in this study, a GPU card is needed with a large number of cores to bring high resolution and fast applications. The configuration to process the data for this research is as follows:

- CPU: Intel(R) Core(TM) i7-7700K CPU @ 4.20GHz, 4200 Mhz, 4 Core(s)
- RAM: 32768 MB (total)
- GPU: NVIDIA GeoForce GTX 1080

The computer used to run these processes is well above the advanced configuration and should not come into any issues with data processing.

Basic configuration up to 32 GB RAM	Advanced configuration up to 64 GB RAM	Extreme configuration more than 64 GB RAM
CPU: Quad-core Intel Core i7 CPU, Socket LGA 1155 (Sandy Bridge, Ivy Bridge or Haswell)	**CPU:** Six-core Intel Core i7 CPU, Socket LGA 2011 (Sandy Bridge-E)	For processing of extremely large data sets a dual socket **Intel Xeon Workstation** can be used.
Motherboard: Any LGA 1155 model with 4 DDR3 slots and at least 1 PCI Express x16 slot	**Motherboard:** Any LGA 2011 model with 8 DDR3 slots and at least 1 PCI Express x16 slot	
RAM: DDR3-1600, 4 x 4 GB (16 GB total) or 4 x 8 GB (32 GB total)	**RAM:** DDR3-1600, 8 x 4 GB (32 GB total) or 8 x 8 GB (64 GB total)	
GPU: Nvidia GeForce GTX 780 or GeForce GTX 980 (optional)	**GPU:** Nvidia GeForce GTX 780 Ti, GeForce GTX 980 or GeForce GTX TITAN X	

TABLE 6: Configuration recommendations from Agisoft (Shervais, 2015).

The typical workflow for processing images in SfM is as follows:

1. Begin 'New Photoscan project'
2. Add photos that will be used for further processing into Agisoft Photoscan Professional software
    a. Separate photos into 'chunks' where each chunk is labeled a different set of flight variable conditions, as seen in Table 4
3. Align photos – using command from Workflow menu
    a. High Quality setting up scales the image by a factor of 4, this setting is recommended for sharp image data for research purposes regarding detailed accuracy
4. Optimize Alignment
5. Build Dense Point Cloud – using command from Workflow menu
    a. Using Ultra high quality – increases processing time but provides greater detail
6. Place markers on GCP's
    a. Zoom in and right click on center of each GCP and 'Add Marker'
    b. In reference pane, load coordinates to corresponding Marker Points from RTK Receiver (Table 5)
    c. Can also be done by uploading a text file with coordinates listed in excel, shown in Table 4.
        i. Z-values omitted
7. Assign project system
    a. From Ground Control Preferences Icon
8. Build Texture

a. Using ‘Generic mode’, most uniform texture will be created

b. Proper texture mapping can help obtain better visual quality for the model

9. Build DEM

a. DEM is rasterized from the dense point cloud

b. A coordinate system must be chosen for reference

Advanced processing users utilize the batch processing feature so that each portion of the data can be aligned in an orderly and efficient process. This method may be faster but does not give the user a chance to view the data while processing. An example of the resulting data from Agisoft is shown in Figure 13. This figure shows the results of a processed point cloud, with the blue squares representing the camera locations and the black lines displaying the angle the images were shot at from the onboard camera. Figure 13 shows the user’s perspective view of the camera locations and the area of interest from 22 March 2019. This image displays the point cloud processed and ready for export.

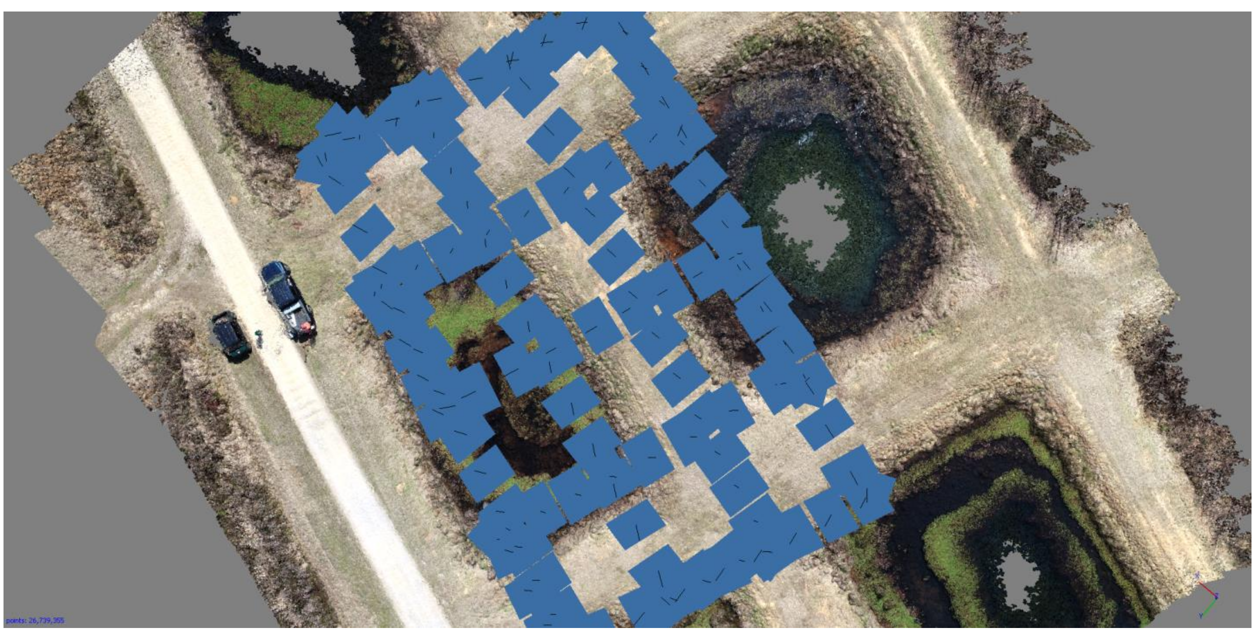

FIGURE 13: User’s view from Agisoft Photoscan software during the post processing phase. Blue squares represent camera locations at 30m above surface.

Point Cloud Creation

The Agisoft algorithm employs SfM techniques to obtain a georeferenced point cloud. The images acquired by the UAS are used to construct a dense 3D point cloud model of the model I-wall using the SfM technique. The simultaneous localization and mapping algorithm (SLAM) reconstructs the camera look angles and scene geometry through automatic alignment and stitching from similar features in each image (James et al., 2012). The algorithm first detects similar points and matches them together from each image. The SLAM algotirhm is capable of augmenting the solution gradually with every new uploaded image (Bobbe et al., 2017). This algorithm comprises of multiple parts: landmark extraction, data association, state estimation, state update, ad landmark update (Riisgaard et al., 2004). The SLAM algorithm tracks and compares these similar features to estimate internal parameters and object coordinates which is then refined iteratively to create a dense point cloud. Then, this algorithm triangulates the matching features and refines the scene (Ridolfi et al., 2017). The SLAM algorithm uses a posterior equation which gives a sequential framework that constantly updates locations of features with a given transfer function. The posterior equation is a probability equation based off discrete and continuous summations. The algorithm is ultimately trying to assume exact knowledge for a position by gathering a sense from various positions and then compute this relative to a world model, assuming a perfect world model. The series of controls is described as u_t and the SLAM algorithm solves for sensor observations o_t over discrete time steps t. The computation derives the UAS's location x_t along with a constant, updated map of the environment m_t (James et al., 2012).

$$P(m_t, x_t | o_{1:t}, u_{1:t})$$

FIGURE 14: SLAM algorithm based off posterior equation. (Ridolfi et al., 2017)

To create a point cloud from oblique images requires a reference plane. The SLAM algorithm is the process in Agisoft Photoscan that automatically aligns and matches images together. This photogrammetry process aligns common features, optimizes the posterior equation while determining the camera locations all within a few minutes, depending on the size of the area of interest. (Bobbe et al, 2017). The posterior equation goes into the motion model which is the prediction step and occurs when the control or measurement is invoked.

After point cloud creation, the point clouds need to be further analyzed for comparison. All processed point clouds were exported into a laser file format (.LAS) and points were georeferenced from the existing GCPs. The resulting analysis is detailed in the results portion. This workflow details how to export the point cloud into XYZ format in Excel® for comparison and analysis.

1. Export each point cloud chunk separately as .LAS file
    a. Precision level set to 9 or higher
2. Import each chunk into Global Mapper for further point cloud comparison
3. Using the 'Path Profile' tool in Global Mapper, display a vertical profile along a specified path using the point cloud data
4. Select a line going perpendicular to the wall
    a. For consistency, select the same area on the wall to create a path profile for every .LAS chunk
5. Path profile tool will display a cross section of the line
    a. Export as points file (XYZ Points)

The software, Global Mapper, was used as a geographic information system (GIS) for accurate point cloud comparison from the points created in Agisoft. A statistical analysis model through Global Mapper will help define and characterize any error of the dense point clouds while comparing each cloud to another. When comparing point cloud, it is important to assess the accuracy and precision of imperfect point cloud for 3D modeling and distinguish the any error.

A method to assess the errors found in point clouds with similar parameters; a clip of the entire wall was taken from Global Mapper. This clip was taken of the entire wall, rather than a perpendicular line. A quantitative analysis should be performed when comparing point clouds to detect the amount of error. This can be done by using any open source point cloud comparison software and inserting two .XYZ files from Global Mapper to measure distances from each other. The CloudCompare software allows the user to insert two point clouds and manually pick equivalent points on both clouds to align them to the same size and shape. This is done by using the automatic transformation matrix given in the program, so that one point cloud will be perfectly matched to the other. At least three pairs of points need to be picked to match the point clouds; more can be added if necessary. This process is repeated for every two sets of point clouds to ensure alignment to further proceed with comparison. As soon as three or more pairs are selected, CloudCompare will show the resulting root mean squared error between the two points. An error contribution will also be shown of each pair, so a new set can be added to replace the worst pair.

CHAPTER IV

RESULTS

Point Cloud Comparison

Each flight had images that were processed into appropriate chunks and their processing time and total amount of points in the dense cloud were noted on the right column of Table 7. From the table, the amount of points derived from each flight acquisition is massive because of the ultra-high, rigorous point cloud setting from Agisoft. The total number of points affected the speed of the processing, shown in the rightmost column of Table 7. Point clouds are a fundamental representation of the surface and can provide location, measurement and 3D information precisely. In a point cloud comparison, each object in the area of interest is recognized, classified, and compared to one another by Agisoft's SLAM algorithm. This study compares one object, the mock I-wall, to itself to see if any movements or displacements can be detected from the point cloud. The study aims to define the edge of the mock I-wall as a way to monitor for change.

TABLE 7: Each data acquisition performed with number of aligned cameras, total dense cloud points, and dense point cloud processing times from the first flights November 08.

Flight	**Look Angle**	**Height**	**Wall Angle**	**Number of Cameras**	**Total Points**	**Point Cloud Processing Time**
1	Nadir	15 m	90°	70	88,353,104	7 hours 9 minutes
2	45°	15 m	90°	44	72,746,848	1 hour 36 minutes
3	Nadir	30 m	90°	54	67,057,806	5 hours 17 minutes
4	45°	30 m	90°	67	93,599,215	10 hours 30 minutes
5	Nadir	15 m	35°	36	71,983,123	1 hour 37 minutes
6	45°	15 m	35°	25	41,497,380	58 minutes 52 seconds
7	Nadir	30 m	35°	28	51,641,444	49 minutes 28 seconds
8	45°	30 m	35°	39	72,940,737	1 hour 19 minutes

It is imperative to note the difference between change detection and deformation analysis. In this approach, change detection requires a straightforward answer – whether or not a movement can be detected from the processed point cloud. A deformation analysis requires an answer of quantity, such as how much movement there was or to identify the movement direction. This study provides a way to interpret and compare point clouds to see if any movement was made.

There are several examples in the literature of comparing UAS-derived point clouds accuracy to number and position of GCP (Harwin and Lucieer, 2012; Lucieer et al, 2013; and Ridolfi et al, 2017). The geolocation of each image provided by the GPS-derived autonomous location and is coded into the header of the imagery. In addition, the platform orientation (yaw, pitch, roll) data from the internal measurement unit (IMU) is also coded into each image file header for relative location calculations conducted during post-processing. To increase accuracy compared to absolute geolocation, GCPs were mapped in the field and captured in the imagery. The coordinate data were transformed from the UTM coordinate system to a coordinate system that aligns to the centerline of the simulated mock wall. The wall axis is orientated approximately northwest to southeast. To simplify the data analysis portion of the project, the entire dataset was rotated clockwise, shown in Figure 15. A rotation is used to perform a rotation in Euclidean space. The rotation matrix for a clockwise rotation also includes the elevation for each point, follows:

$$\begin{bmatrix} UTM_x \\ UTM_y \\ z \end{bmatrix} \cdot \begin{bmatrix} \cos\theta & -\sin\theta & 0 \\ \sin\theta & \cos\theta & 0 \\ 0 & 0 & 1 \end{bmatrix} = \begin{bmatrix} WALL_x \\ WALL_y \\ z \end{bmatrix}$$

$$WALL_x = UTM_y*SIN(\theta*\boldsymbol{\pi}()/180) + UTM_x*COS(\theta*\boldsymbol{\pi}()/180)$$

$$WALL_y = UTM_y*COS(\theta*\boldsymbol{\pi}()/180) - UTM_x*SIN(\theta*\boldsymbol{\pi}()/180)$$

Where θ is the clockwise rotation angle.

FIGURE 15: Rotation matrix used by extracting coordinate values to estimate true location of wall.

Figure 16 a-b are the flight plans that correspond with the point clouds in Figures 17 a-b. In Figure 16, neither flight path flew directly over the wall, which is the cause of distortion in the point clouds, where the point cloud shows parts of the wall that should not be seen in nadir. The layover proves that it is imperative to fly directly over the wall when capturing images in nadir or oblique, to avoid distortion. UAS operators should spend a significant amount of time planning and determining look angles to avoid errors such as layover, seen in Figure 17. Another notable issue is flying directly nadir is not conducive to effectively reconstructing a 3D model from images. Flying only nadir for data collection does not allow the user to capture the sides of the wall accurately. Without entire coverage of the area, the Agisoft algorithms began the make assumptions and estimates points as to avoid gaps within the data. Having a combination of oblique and nadir imagery is advantageous or having oblique imagery in a double grid flight pattern provides the least amount of error in point cloud processing.

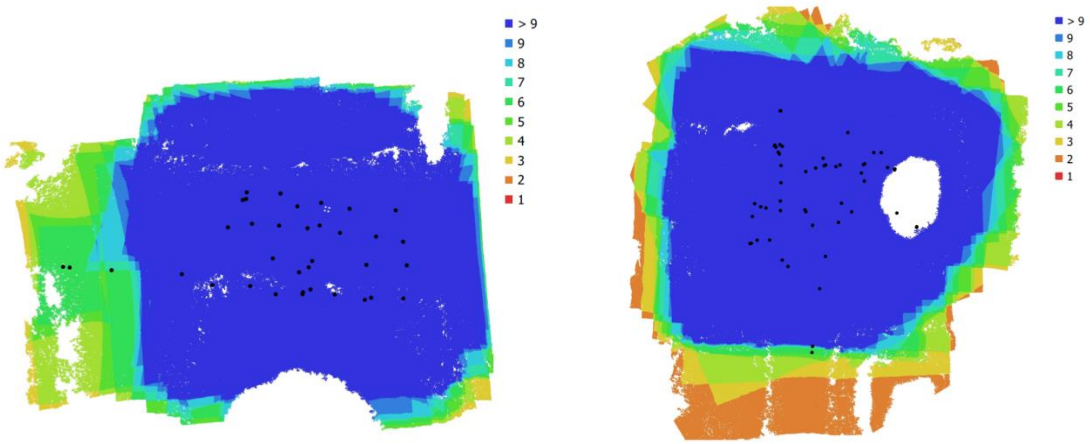

FIGURE 16a-b: Generated processing report from Agisoft Photoscan. (a) Flight path of acquisition 1 corresponding to the point cloud of Figure 17a. (b) Flight path of acquisition 3 corresponding to the point cloud of Figure 17b. Camera locations are denoted by black dots.

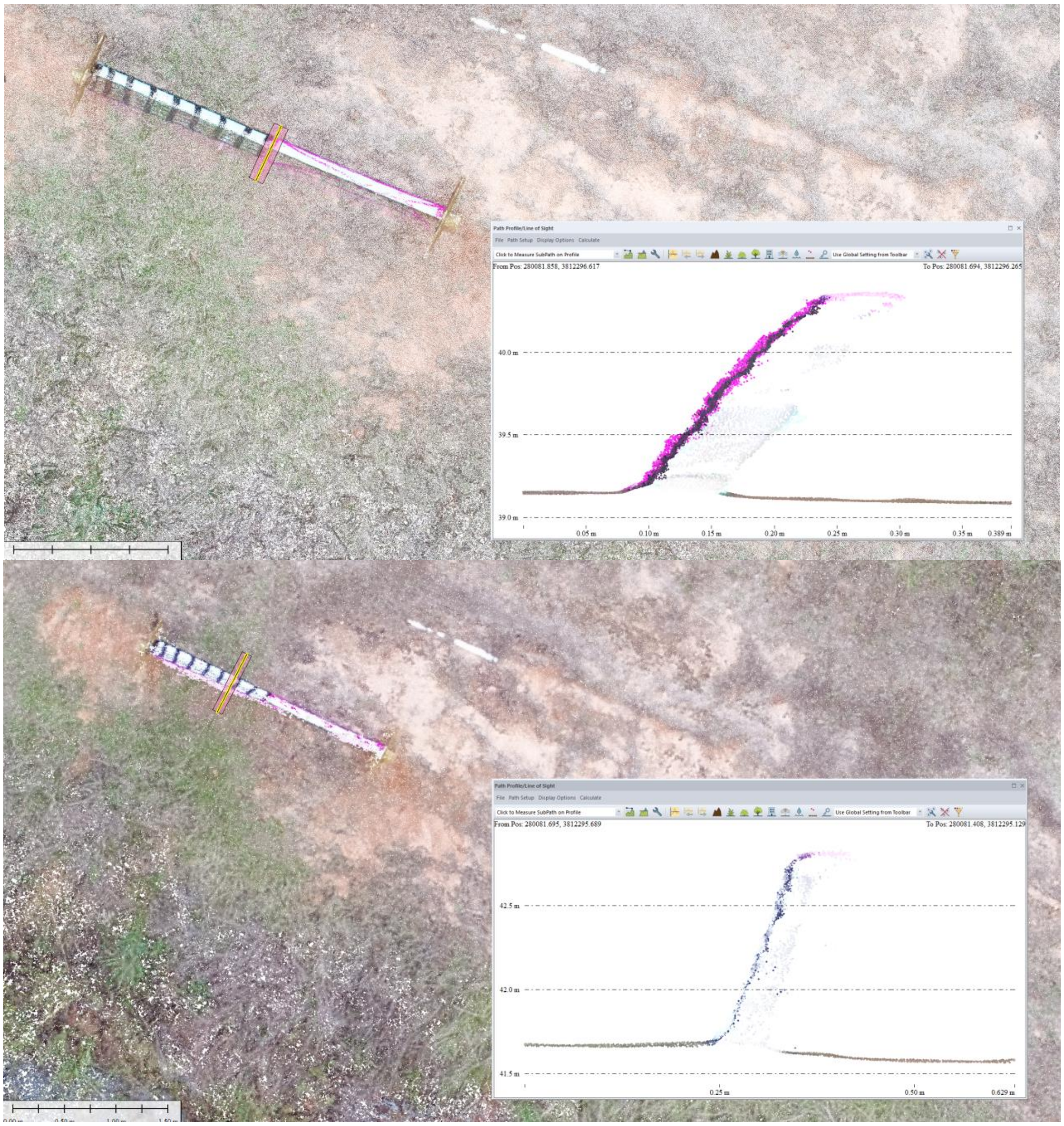

FIGURE 17a-b: Images captured from Global Mapper showing a path profile through the mock I-wall. (a) Path profile of flight acquisition 1. (b) Path profile of flight acquisition 3.

Using the photogrammetric range imaging technique, also known as SfM, point clouds can be created from oblique and nadir imagery and then further analyzed for comparison. It is important to note that it is seldom obtainable to find “true nadir” because of unavoidable angular rotations caused by the attitude of the UAS at the instant of exposure. These miniscule tilts cause a difference of about 1-3 degrees from vertical therefore assuming all imagery is slightly tilted.

The results from the first experiment were evaluated, changes to the data collection procedure were made repeated to gain more accurate results to try and clearly see the edge of the mock I-wall in the point cloud. Shadows were cast because of the solar procession and can be clearly seen in Figure 18 a-b. Although shadows were present, data quality was not affected entirely since the focus was the height on the wall. The view of the point cloud in Global Mapper is nadir therefore the sides of the mock I-wall should not be seen from this angle. Results from the repeated experiment show the edge of the wall more clearly defined in the onset graph of each image. In Figure 18 a-b, the edge and top of the wall are clearly delineated. This can be attributed to improved flight parameters such as a greater overlap percentage, oblique angles only, a double grid flight plan mission (Pix4D), and an added GCP to help define the reference frame. It has been well documented (Kubota, 2017) that additional GCPs improve the accuracy of a project. Additional flight paths and look angles will increase the time requirements and processing time but a better product is created. An optimization of the first flight acquisition parameters was needed. The mock I-wall was not manually tilted because the focus of the second flight set was to see the edge of the wall at 90 degrees. It is difficult to maintain absolute accuracy in the field; many cloud comparison soft wares become too cumbersome for the scope of this project. The focus was shifted to the simple detection of the edge of the mock I-wall, so it was not tilted for the purpose of this research.

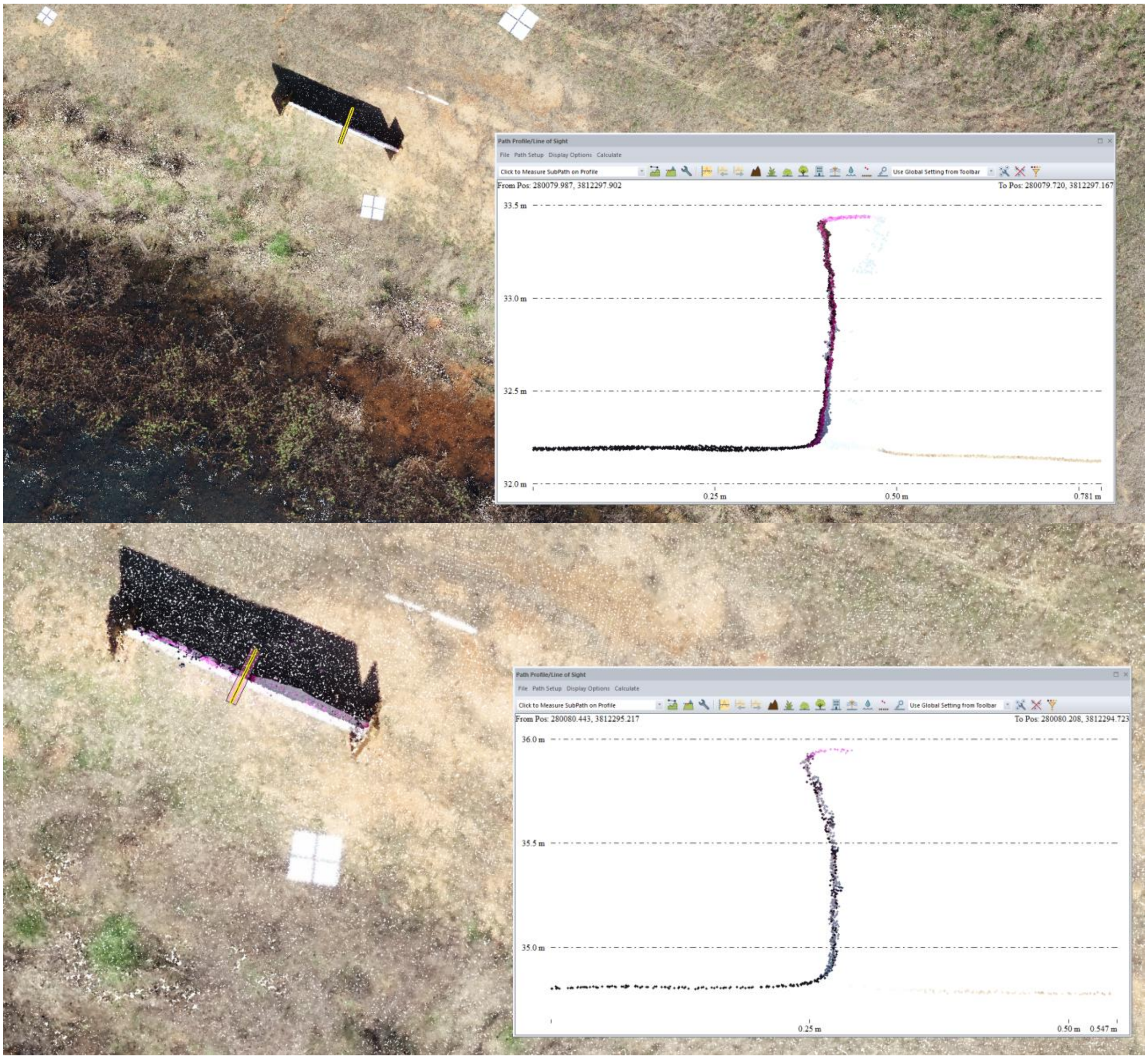

FIGURE 18a-b: Images from second data collection in Global Mapper. (a) Path profile of flight acquisition of 3a. (b) Path profile of flight acquisition 4a.

The methods were again simulated on an actual floodwall structure found in Oxford, Mississippi. The methods proved to be successful in defining the clear surfaced of the floodwall structure through the point clouds in Global Mapper. Figure 19 a-b shows a path profile taken from two different areas on the point cloud. Results show the point clouds are not completely vertical which can be attributed to a variety of reasons. Figure 19a shows a fairly vertical cross section and the slight tilt can be characterized from heavy shadows or not enough camera angles to produce an accurate 3D cloud. The right side of the cross sectional area of Figure 19b is attributed to flowing water and distorted the point cloud for the wall on that side.

FIGURE 19 a-b: Path profile tool used on two different parts of the floodwall structure. Path profile outlined in red. (a) Cross sectional area of wall, measured 1/4th inch from vertical. (b) Cross sectional area of different area of wall, measured 1 1/4th inch from vertical.

Multispectral Analysis

The multispectral analysis proved to be an addition to investigate finite features of a sharp edge. The RedEdge-M is a durable attachment that can be integrated onto a UAS to capture five narrow spectral bands. An experiment was run with the RedEdge-M multispectral camera kit and results show the edge of a wall can be clearly detected with a high contrasting feature, such as a reflective tape, and low altitude. The RedEdge-M will not be attached to the UAS for the purpose of this research because the equipment blocks the obstacle sensor on the UAS. Multispectral tools should still be considered for future research.

Error Analysis

Results from the second flight acquisition show the current technology can capable of capturing the surface of the wall at as millimeter level. Errors arise from defining where the surfaces meet at an edge. Instead of defining a point or a surface to compare, future work may focus towards temporal analysis to discover more detail about movement.

Point pair registration is crucial to align point clouds and further perform any error analysis. In the CloudCompare software, once the point clouds are aligned, the cloud-to-cloud distance can be performed. This tool allows each point to be compared to one another from the *compared cloud* to the *reference cloud*. These points are averaged into a mean and standard deviation show in Table 8. The point clouds compared will have the same parameters. This quantitative analysis allows the user to identify how large the error may be, based off the similar camera and look angle parameters. Point clouds 1 and 5 from flight acquisition 1 have the worst mean value; this can be attributed to the issues found in the flights with the nadir look angle creating a large distortion in the point clouds.

TABLE 8: Error analysis performed by comparing point clouds to each other.

Point Clouds Compared	**Flight Acquisition**	**Mean**	**Standard Deviation**
2a and 4a	2	0.026641	0.027081
1 and 5	1	0.148128	0.148122
2 and 6	1	0.022559	0.022555
4 and 8	1	0.017847	0.013132

One of the main factors affecting accuracy is resolution of the images which refers to the number of pixels in an image or the amount of detail an image can hold. A higher resolution is better for detailed imagery. If this were to be improved upon, an issue would still lie with the shutter speed of the camera. The DJI Phantom 4 Pro has a mechanical shutter speed of 8-1/2000s and when not in a flight plan with designated parameters, the images have a chance of being blurry and therefore cannot be processed. A faster shutter speed could allow the UAS to travel at a faster velocity and still capture clear images to reconstruct a 3D model.

Another important factor to maintain accuracy in photogrammetry is to calibrate the UAS camera before any flight. The calibration process determines the camera focal length and fixes any lens distortion. Accuracy will be lower if the onboard camera is not properly calibrated according to the manufactures guide. Diverse camera angles and positions are another factor in maintaining a high level of accuracy. SfM modeling involving 360° of coverage for the object of interest is hard to achieve when solely processing nadir imagery. Oblique imagery corrects distortions in point clouds and corrects layovers, as seen in Figure 17 a-b. When the data process was repeated on 22 March 2019, a 70° camera angle was used for all four flight acquisitions and proved to be successful for capturing the defined edges of the wall.

The “cross-hatch” pattern is optimal for collecting imagery in nadir or oblique. Pix4D offers a double grid mission and the angles of the grids can be altered for better coverage of the study area. If the area is fairly flat-lying with not much ground variation, any flight pattern can be used. For ideal data and imagery, UAS should follow their optimal flight pattern depending on the outcome the user is looking for. This cross-hatch pattern is illustrated from a data set in behind the Oxford Fire Station #3 in Figure 20. This figure also displays error estimates given by camera locations in a generated report by Agisoft. The Z error is represented by the ellipse color and X, Y errors are represented by the ellipse shape. The error average vertically is consistent for each row and varying horizontally. The grid is slightly tilted over the floodwall structure to capture better imagery of the sides for depth.

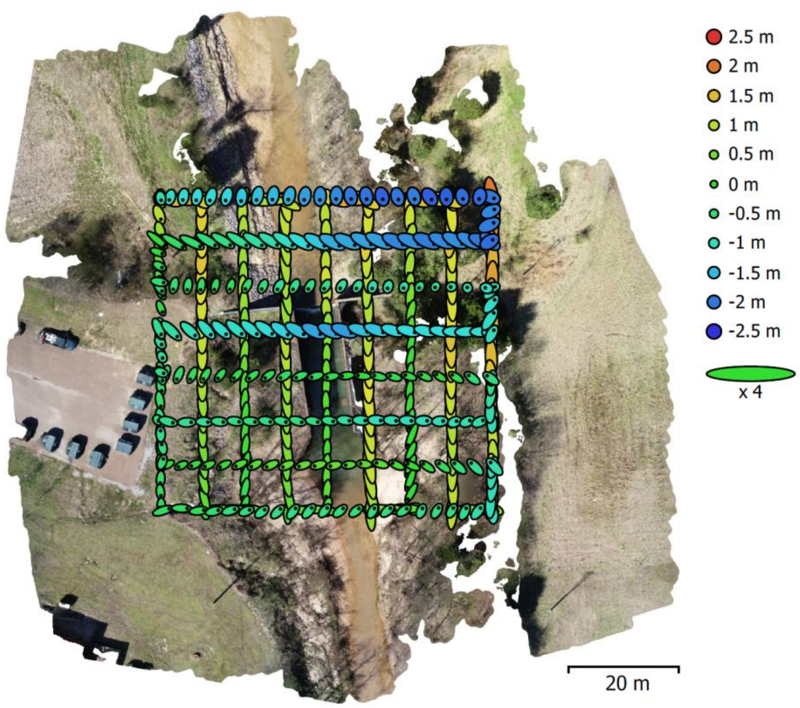

FIGURE 20: Camera locations and error estimates. Z error is represented by ellipse color. X, Y errors represented by ellipse shape.

CHAPTER V

DISCUSSION & CONCLUSION

The conclusion is that UAS-based imagery in combination with SfM principles and image correlation algorithms can provide versatile and effective tools when monitoring displacement at a centimeter level. In this study, a UAS was used to collect multivariable sets of high resolution images over a constructed model I-wall at the UMFS. SfM was used to convert images into 3D dense point clouds and DEMs. The aim was to visually detect displacement of an I-wall by capturing images at a different angle and height and outlining the edge of a mock I-wall. The SLAM algorithm was successful in quantifying the displacement but the scale of the study is too small for this application.

The study provides evidence of using UAS as a way to inspect a floodwall structure and several conclusions can be derived from this research project. For future applications, using the methods outlined here in conjunction with other data such as vegetation contrast and multispectral identification could lead to more accurate 3D reconstruction models.

Results from this study suggest the point clouds need to have various camera angles and lower elevation to effectively capture the edges of the wall. The height can be problematic depending on where the floodwall infrastructure is located. Many obstacles can hinder the UAS from entering in the location safely, such as powerlines, neighboring tall vegetation, and other overhead obstacles. There are certain limitations to access obtainable accuracy for measuring and monitoring walls. The wall surfaces can be observed from a combined view of oblique and nadir images. In the first analysis, all nadir images that captured the wall were distorted and revealed a layover effect that assumed the wall to be thicker than it is. These nadir images did not fly directly above the wall so this causes an exaggeration of the point cloud to compensate for the unknown space that the camera did not observe properly. The dominant factor affecting the data quality seems to be the need of a higher ground resolution or higher caliber camera.

If this study were to be performed again, the object in question would have more contrast. The higher contrast would make the point clouds more defined and easier to filter out outliers and errors that would distort the data. Another addition would be including more GCPs into the study. There would be more GCPs placed along important features of the wall or on the top of the highest points. More GCPs would help Agisoft georeference the dense point cloud into a 3D model. The impact of well-placed GCPs could affect the accuracy of the resulting model; the model accuracy can then increase reliability when creating a survey operation. The size of the model I-wall would also need to increase in thickness. The current model I-wall was very thin but it was similar to sheet pile web thickness. The capabilities of the UAS and software required a thicker wall with known verticality.

Methods proposed in this study are low cost and can be performed by any recreational UAS user. These methods can also be used in applications other than I-wall monitoring for displacement. The workflow provided can be used to assess difference types of movement of an object or scene from imagery captured from a UAS. By building both ultra-high dense point clouds and DEMs, the applications within a temporal scale are endless. With the addition of SfM, the 3D nature of certain features can highly detail with ease of use.

Results indicate combined use of UAS and SfM can be used to measure movement or displacement of a small mock I-wall structure. The choice any additional technologies are up the decision of the user, the size and proportions of the area, and will depend on the available budget. This study demonstrated that a recreational UAS can be used to create point clouds at a centimeter scale, but failed to clearly denote differences in the wall angles. This study provides a platform to further the opportunity to capture high resolution 3D information on an area to record small displacements.

There were some existing outlier points in most of the points from the point clouds in Global Mapper. In Agisoft, it can be seen that the wall with the black duct tape has some points projected inwards while the pink duct tape showed some points projecting outwards. These outlier points can cause error and some vagueness when analyzing the top or side edge of the wall. These points are from Agisoft's SLAM algorithm trying to tie the points together and assuming the location of each. In the preliminary flight acquisition, the blank white surface of the original mock I-wall fooled the feature detection algorithm and caused no tie points to be detected in that vicinity. If this study were to be repeated, infrared tape would be placed on the edge of the wall and a multispectral attachment would be affixed to the UAS. Multispectral techniques aid in the clarity of distinguishing a sharp edge on the wall. A multispectral enhances the contrast between the vegetation on the surface and the wall so many outlier points could be eliminated.

Based on the failure types of the floodwall structures in New Orleans from Hurricane Katrina, this research aims to detect movement using a UAS of a wall to observe if there is a lean to preemptively mitigate any geohazards. A temporal analysis is the most practical process to view this type of displacement from a real floodwall structure. A temporal analysis has the ability to describe patterns based on time and different environmental conditions to view subtle changes by smaller time-based increments. Knowing the floodwall structure is completely vertical helps the user define a temporal analysis using UAS and SfM because the displacements will be shown off 90°, an established constant.

Real World Applications

The motivation for this research was the I-wall failures that occurred during Hurricane Katrina in New Orleans. Applications were used and simulated through this study to try and detect movement from a mock I-wall to then translate to a real wall. The narrow dimension of the mock I-wall introduced errors while post processing and the lack of contrast made it difficult to distinctly characterize the edges of the wall. This led to the invitation to capture images at a real floodwall structure behind Fire Station #3 in Oxford, Mississippi. Using the methods and applications from the mock I-wall at the UMFS, images were captured at a new location with an actual floodwall structure. The floodwall structure should be completely vertical but was leveled off for assurance. The floodwall was a 1/4th inch off from vertical in some areas and 3/8th inch in others. This was measured in the field using a level. The UAS performed a double grid mission over the area in a designated bounding box, at a 30 m altitude and 70° oblique look angle.

Temporal analysis of data can help a user define patterns and examine the behavior of the variable wall in a data set over time. Applying a temporal analysis to the research of an actual floodwall can aid the process of defining a clear edge of a wall. Over time, data can be combined or compared to one another to view if the floodwall structure has shifted and in which direction. Further investigations could use these multi-temporal datasets and functions based off of a frequency domain, rather than a spatial domain. If each data set was taken every week at the same time, these resulting point clouds could be amalgamated to completely define the object in question. Adding more points results in a stronger, more complete dataset in hopes of discovering movement. The detection of the edge of the mock I-wall proved to be difficult because of the limited frame space, but the methods used remain consistent to estimate 3D structure from a 2D sequence of images.

In the growing field of photogrammetry, UAS are becoming more powerful and of higher caliber. A temporal analysis becomes more feasible because newer UAS can sustain a longer battery life and continue to capture high quality images with significant overlap. A temporal analysis will help determine the frequency of collection to allow for faster flight speeds and higher altitudes while still yielding reasonable results. Although these types of studies have been performed on infrastructure or urban buildings, not much research has been done on floodwall structures, more specifically I-walls.

LIST OF REFERENCES

REFERENCES

Aicardi, I., Chiabrando, F., Grasso, N., Lingua, A. M., Noardo, F., & Spanó, A. (2016). UAV photogrammetry with oblique images: First analysis on data acquisition and processing. *International Archives of the Photogrammetry, Remote Sensing and Spatial Information Sciences - ISPRS Archives*, *2016–Janua*, 835–842. https://doi.org/10.5194/isprsarchives-XLI-B1-835-2016

Bemis, S.P., Micklethwaite, S., Turner, D., James, M.R., Akciz, S., Thiele, S.T., Bangash, H.A. (2014). Ground-based and UAV-based photogrammetry: A multi-scale, high-resolution mapping tool for structural geology and paleoseismology. Journal of Structural Geology 69, 163–178. https://doi.org/10.1016/j.jsg.2014.10.007

Brauneck, J., Pohl, R., & Juepner, R. (2016). Experiences of using UAVs for monitoring levee breaches. IOP Conference Series: Earth and Environmental Science, 46(1), 0–6. https://doi.org/10.1088/1755-1315/46/1/012046

Cheuk, C. Y., White, D. J., & Bolton, M. D. (2005). Deformation mechanisms during uplift of buried pipes in sand. *16th ICSMGE*, *0241*(May), 1685–1688. https://doi.org/10.1061/(ASCE)1090-0241(2008)134

Choung, Y. (2014). Mapping levees using LiDAR data and multispectral orthoimages in the Nakdong River Basins, South Korea. *Remote Sensing*, *6*(9), 8696–8717. http://doi.org/10.3390/rs6098696

Comfort, L. K. (2006). Cities at risk: Hurricane Katrina and the drowning of New Orleans. *Urban Affairs Review*, *41*(4), 501–516. https://doi.org/10.1177/1078087405284881

Dixon, T. H., Amelung, F., Ferretti, A., Novali, F., Rocca, F., Dokka, R., & Whitman, D. (2006). Space geodesy: Subsidence and flooding in New Orleans. *Nature*, *441*(7093), 587–588. https://doi.org/10.1038/441587a

Duncan, J. M., Brandon, T. L., Wright, S. G., & Vroman, N. (2008). Stability of I-Walls in New Orleans during Hurricane Katrina. *Journal of Geotechnical and Geoenvironmental Engineering*, *134*(5), 681–691. https://doi.org/10.1061/(ASCE)1090-0241(2008)134:5(681)

FEMA Levee Resources and Library. (2017). Available online: http://www.fema.gov/living-levees-itsshared-responsibility/fema-levee-resources-library (accessed on 4 May 2018).

Fisher, W.D., Camp, T.K., & Krzhizhanovskaya, V.V. (2016). Crack detection in earth dam and levee passive seismic data using support vector mechanics. *The Internatioal Conference on Computational Science, 80,* 577-586.

Fraser, B., Congalton, R., Fraser, B. T., & Congalton, R. G. (2019). Evaluating the Effectiveness of Unmanned Aerial Systems (UAS) for Collecting Thematic Map Accuracy Assessment Reference Data in New England Forests. *Forests*, *10*(1), 24. https://doi.org/10.3390/f10010024

Fujita, Y., Hoshino, Y. Kobayashi, I., and Mizuno, J. (2015). Consideration for River CIM Management Model Using Combination of Various Existing Data, Journal of Japan Society of Civil Engineers Division F3: Civil Engineering Informatics, Vol. 71, No. 2, pp. 1_79-1-86.

Harwin, S., & Lucieer, A. (2012). Assessing the accuracy of georeferenced point clouds produced via multi-view stereopsis from Unmanned Aerial Vehicle (UAV) imagery. *Remote Sensing*, *4*(6), 1573–1599. https://doi.org/10.3390/rs4061573

Hughes, S. A., & Nadal, N. C. (2009). Laboratory study of combined wave overtopping and storm surge overflow of a levee. *Coastal Engineering*, *56*(3), 244–259. http://doi.org/10.1016/j.coastaleng.2008.09.005

Independent Levee Investigation Team. (2006). Chapter Three: Geology of the New Orleans Region, *1*, 1–50.

Jagt, B., Lucieer, A., Wallace, L., Turner, D., & Durand, M. (2015). Snow Depth Retrieval with UAS Using Photogrammetric Techniques. *Geosciences*, *5*(3), 264–285. https://doi.org/10.3390/geosciences5030264

James, M. R., & Robson, S. (2012). Straightforward reconstruction of 3D surfaces and topography with a camera: Accuracy and geoscience application. *Journal of Geophysical Research: Earth Surface*, *117*(3). https://doi.org/10.1029/2011JF002289

Kliche, Charles A. (1999), *Rock Slope Stability*, Colorado, USA: Society for Mining, Metallurgy, and Exploration, *ISBN 0-87335-171-1*

Kubota, S., Kawai, Y., & Kadotani, R. (2017). Accuracy validation of point clouds of UAV photogrammetry and its application for river management. International Archives of the Photogrammetry, Remote Sensing and Spatial Information Sciences - ISPRS Archives, 42(2W6), 195–199. https://doi.org/10.5194/isprs-archives-XLII-2-W6-195-2017

Lee, J.S. (2010). River Engineering and Design; Saeron Books: Seoul, Korea. *Environmental Earth Sciences*, 1687–1694.

Lucieer, A., Jong, S. M. d., & Turner, D. (2014). Mapping landslide displacements using Structure from Motion (SfM) and image correlation of multi-temporal UAV photography. *Progress in Physical Geography*, *38*(1), 97–116. https://doi.org/10.1177/0309133313515293

Lillesand, T.M., Kiefer, R.W., Chipman, J.W.(2004). *Remote Sensing and Image Interpretation, 5th edition.* Hoboken, NJ: John Wiley & Sons, Inc.

Madden, M., Jordan, T., Bernardes, S., Cotten, D. L., Hare, N. O., & Pasqua, A. (2015). Unmanned Aerial Systems and Structure from Motion Revolutionize Wetlands Mapping, (April). https://doi.org/10.1201/b18210-13

Martínez-Espejo Zaragoza, I., Caroti, G., Piemonte, A., Riedel, B., Tengen, D., & Niemeier, W. (2017). Structure from motion (SfM) processing of UAV images and combination with terrestrial laser scanning, applied for a 3D-documentation in a hazardous situation. *Geomatics, Natural Hazards and Risk*, *8*(2), 1492–1504. https://doi.org/10.1080/19475705.2017.1345796

Prosdocimi, M., Calligaro, S., Sofia, G., Dalla Fontana, G., Tarolli, P., Schenk, T., … Lane, S. N. (2015). Structure from Motion (SfM) Photogrammetry Photogrammetric heritage. *Department of Civil and Environmental Engineering and Geodetic Science, The Ohio State University*, *40*(14), 79–95. https://doi.org/10.1002/esp.3767

Rebolj, D., Pučko, Z., Babič, N. Č., Bizjak, M., & Mongus, D. (2017). Point cloud quality requirements for Scan-vs-BIM based automated construction progress monitoring. *Automation in Construction*, *84*(October), 323–334. https://doi.org/10.1016/j.autcon.2017.09.021

Relationship, I. T. S., & Land, T. O. (2000). Geology of Greater New Orleans. *Environmental Earth Sciences*, 1687–1694.

Ridolfi, E., Buffi, G., Venturi, S., & Manciola, P. (2017). Accuracy analysis of a dam model from drone surveys. *Sensors (Switzerland)*, *17*(8). https://doi.org/10.3390/s17081777

Riisgaard, S., & Blas, M. R. (2004). SLAM for Dummies. *A Tutorial Approach to Simultaneous Localization and Mapping, 22*(June), 1-127.

Rocscience, Inc.(2005). Slide v5.0—2D limit equilibrium slope stability analysis, Toronto.

Rodgers, J. (2009). Geological Conditions Beneath the New Orleans Area. Retrieved from http://web.mst.edu/~rogersda/levees/Geology New Orleans-Chapter 3.pdf

Rossi, P., Mancini, F., Dubbini, M., & Mazzone, F. (2017). Combining nadir and oblique UAV imagery to reconstruct quarry topography : methodology and feasibility analysis. *European Journal of Remote Sensing*, *50*(1). https://doi.org/10.1080/22797254.2017.1313097

Schleifstein, M. (2006). What is an I-wall? *The Times-Picayune.* Advance Local Media, 06 June 2017. https://www.nola.com/environment/index.ssf/2017/06/what_is_an_i-wall.html

Seed, R. B., Asce, M., Bea, R. G., Asce, F., Asce, S. M., Boutwell, G. P., Cheung, C. (2008). New Orleans and Hurricane Katrina. II : The Central Region and the Lower Ninth Ward. *Journal of Geotechnical and Geoenvironmental Engineering*, *134*(5), 718–740. https://doi.org/10.1061/(ASCE)1090-0241(2008)134:5(718)

Shervais, K., & Dietrich, J. (2016). Structure from Motion (SfM) Photogrammetry Data Exploration and Processing Manual, 1–28.

Shervais, K. (2016). Structure from Motion guide for instructors and investigators, 1–24.

Sills, G. L., Asce, M., Vroman, N. D., Wahl, R. E., Asce, M., & Schwanz, N. T. (2008). Overview of New Orleans Levee Failures : Lessons Learned and Their Impact on National Levee Design and Assessment, (May), 556–565.

Smith, D. P., & Atkinson, S. F. (2001). Accuracy of rectification using topographic map versus GPS ground control points. *Photogrammetric Engineering and Remote Sensing*, *67,* 565–570 ST–Accuracy of rectification using topo. Retrieved from https://www.asprs.org/wp-content/uploads/pers/2001journal/may/2001_may_565-570.pdf

US Army Corps of Engineers, National Levee Database. http://nld.usace.army.mil/egis/f?p=471:1:

Ubilla, J., Abdoun, T., Sasanakul, I., Sharp, M., Steedman, S., Vanadit-Ellis, W., & Zimmie, T. (2008). New Orleans Levee System Performance during Hurricane Katrina: London Avenue and Orleans Canal South. *Journal of Geotechnical and Geoenvironmental Engineering*, *134*(5), 668–680. https://doi.org/10.1061/(ASCE)1090-0241(2008)134:5(668)

Ullman, S. and Brenner, S. (1988) The Interpretation of Structure from Motion. **203**. *Proceedings of the Royal Society of London. Series B. Biological Sciences.*

USACE. (2006). Distribution Restriction Statement. *Engineer*, *EM 200-1-1*(200), 1–499.

USACE. (2007). Elevations for Design of Hurricane Protection Levees and Structures, (December), 1–269.

USACE. (2009). The 17th Street Canal breach in New Orleans after Hurricane Katrina. *PRI's The World,* Jeb Sharp, OZY Media News, 14 August 2015. https://www.pri.org/stories/2015-08-14/ten-years-later-lessons-hurricane-katrina-apply-all-us

U.S. Army Corps of Engineers. (1989). “Retaining and Floodwalls,” Engineering Manual 1110-2-2502, HQUSACE Engineering and Design, Washington, DC.

U.S. Army Corps of Engineers. (2005). “Stability Analysis of Concrete Structures,” Engineering Manual 1110-2-2100, HQUSACE Engineering and Design, Washington, DC.

U.S. Army Corps of Engineers. (2009). “Performance Evaluation of the New Orleans and Southeast Louisiana Hurricane Protection System – Final Report of the Interagency Performance Evaluation Task Force,” Volume VIII – Engineering and Operational Risk and Reliability Analysis, Interagency Performance and Evaluation Task Force, New Orleans, LA.

U.S. Army Corps of Engineers. (2011). “Evaluation of I-Walls,” Engineering Technical Letter 1105-2-575, HQUSACE Engineering and Design, Washington, DC.

U.S. Army Corps of Engineers. (2012). “Levee Screening Tool – Methodology and Application,” Technical Users Reference Manual RMC-CPD-1, Risk Management Center, Golden, CO.

van Heerden, I., Bryan, M. (2006). *What Went Wrong and Why: During Hurricane Katrina. Viking. ISBN 0-670-03781-8.* https://web.archive.org/web/20110807184732/http://levees.org/2/wp-content/uploads/2010/06/American-Society-of-Civil-Engineers-What-Went-Wrong-ERPreport-1.pdf

Verhoeven, G. (2011). Taking computer vision aloft – archaeological three-dimensional reconstructions from aerial photographs with photoscan: Arcchaeological Prospection, v. 18, p. 67-73.

Wallace, L., Lucieer, A., Malenovskỳ, Z., Turner, D., & Vopěnka, P. (2016). Assessment of forest structure using two UAV techniques: A comparison of airborne laser scanning and structure from motion (SfM) point clouds. *Forests*, *7*(3), 1–16. https://doi.org/10.3390/f7030062

Wang, C., Cho, Y. K., & Kim, C. (2015). Automatic BIM component extraction from point clouds of existing buildings for sustainability applications. *Automation in Construction*, *56*, 1–13. https://doi.org/10.1016/j.autcon.2015.04.001

VITA

Eleanor Dietz received a Bachelor of Science degree in Geology at the University of Houston. Graduating a semester early in 2016, Eleanor began applying to graduate schools. In 2017, she attended graduate school at The University of Mississippi in Oxford, Mississippi, where she obtained her Master of Science degree in Geological Engineering in May of 2019. She has also been awarded the Dawn Blackledge Scholarship in the spring of 2019 from the University of Mississippi. Eleanor is now working as an underground mining geotechnical engineer in Elko, Nevada.